

The Structural Organization of the Ventral Posteriorolateral Nucleus in the Rat

J.P. MCALLISTER AND J. WELLS

Department of Anatomy and Neurobiology, University of Vermont, Burlington, Vermont 05405

ABSTRACT The structural plan of the ventral posterolateral nucleus (VPL) in the rat was analyzed by using a variety of techniques to study the pattern of distribution of the ascending afferent fibers and the synaptology of the neuropil within this somatosensory relay nucleus. Golgi stains, Fink-Heimer methods, HRP labeling methods, and electron microscopy were all used in the analysis.

The neurons in VPL are aligned in rostrocaudal and dorsoventral rows that are roughly parallel to the curvature of the external medullary lamina (EML) and curve partially around the rostral pole of the ventral posteromedial nucleus (VPM). Golgi-impregnated sections reveal that the dendritic trees of the VPL neurons conform in general to the laminar pattern of VPL. Thick proximal dendrites extend about 25 μm from the cell bodies. Most proximal dendrites are aligned with the laminae of VPL but the distal dendrites spread over many laminae within VPL. The inputs from the dorsal column nuclei (DCN) end only on proximal dendrites as large, round-vesicle terminals. About 20–25% of the small round-vesicle terminals originate in the cerebral cortex and synapse only on the distal dendrites. The third type of synapse contains many flattened vesicles and is of unknown origin. No serial synapses or vesicle-containing dendrites were observed. Input from the spinal cord projects to two segregated zones which are transitional between the ventral lateral nucleus (VL) and VPL rostrally and between the posterior thalamic complex (PO) and VPL caudally. Each transition zone contains neurons characteristic of both VPL and the adjacent region. Ascending afferent projections were demonstrated by the anterograde transport of HRP following injections into the ventral mesencephalon and by Fink-Heimer stains of degeneration resulting from small lesions of the DCN. Both methods indicate that large-caliber axons course parallel to each other and give off collaterals that diverge to widespread areas of the VPL. The widespread terminal fields that result do not conform to the laminar pattern of the nucleus. Small punctate lesions of DCN result in sparse degeneration that is also widespread in VPL. Structures which appear to be clusters of terminal arborizations of the ascending afferent input were also observed in VPL. These results suggest that somatotopy and modality separation in VPL may be determined either by intrinsic and/or corticothalamic morphological relationships and not by precise topographical ordering of sensory input.

The structural organization of a projection nucleus in many ways determines the physiological strategies that the neurons use to convert the inputs into outputs while maintaining the significant features of the processed information. Few regions of the mammalian brain have such an uncomplicated organization that they can be studied in enough detail to allow formulation of a complete structural plan that explains the mechanisms of the relay of

information through the region. The rat ventral posterolateral nucleus (VPL) may have the kind of relatively simple structure that will facilitate such studies. We are attempting to determine a structural plan that is as complete as possible for VPL of the rat in order that we may analyze the processing of somatosensory

J.P. McAllister's present address is Mental Retardation Research Center, UCLA, Los Angeles, CA 90024.

Reprint requests should be addressed to J. Wells.

information at this thalamic site and study the structural reorganization of the cortical and lemniscal inputs to VPL following deafferentation (Donoghue and Wells, '77; Tripp and Wells, '78).

Many of the details of the structural plan for VPL found in the literature are related to the VPL of the cat and are often described in terms of the ventrobasal complex (VB), which includes both ventral posteromedial nucleus (VPM) and VPL. The importance of differentiating between the two nuclei has been emphasized in our initial Golgi studies (McAllister et al., '78) which have indicated that VPL neurons were distinctly different from those usually ascribed to VB (Scheibel and Scheibel, '66a,b; Ramón y Cajal, '66). In addition, the existing studies of VB/VPL in the rat have indicated that the rat has a markedly different structural organization from that of the cat. For example, the rat VB may not have intrinsic or local circuit neurons (Scheibel and Scheibel, '66a,b; Ramón y Cajal, '66) nor synaptic arrangements that are thought to provide pre-synaptic inhibition or surround inhibition, i.e., serial synapses and vesicle-containing dendrites (Spacek and Lieberman, '74; Matthews and Faciane, '77; Tripp and Wells, '78). Both kinds of arrangements and their functional implications have been described for the cat (Ralston and Herman, '69; Ralston, '71) and greatly influence theories of the relay of somatosensory information through the thalamus. The rat VPL uses a different and, we suspect, a less complex structural arrangement to carry out basically the same task as the cat VPL. The suspected simplicity, relative to other species (Ralston and Herman, '69) and to other relay nuclei in the rat (Lieberman, '73), also led us to believe that a more complete plan could be determined for the rat than for the more complicated structural arrangements in the cat.

Previous studies have described a structural lamination of VB (Scheibel and Scheibel, '66a,b) and suggest this pattern is related to its function in the relay of somatosensory information from the spinal cord and dorsal column nuclei (DCN) to the cerebral cortex. The terminal arbors of the lemniscal input were described as conforming to an "onionskin" as if there were structurally dependent circuits necessary for the relay of the input information, i.e., a cell in DCN projecting to a certain point within one lamina of the onionskin. On the output side of the VPL projection, recent studies in the rat by Saporta and Kruger ('77)

support the concept of lamination in VB by showing that points in the somatosensory cortex receive projections from coherent bands of neurons within VB. None of these studies in the rat have addressed the problem of the collateralization of the lemniscal input although collaterals were shown in the illustrations of the Golgi studies (Scheibel and Scheibel, '66a,b; Ramón y Cajal, '66). It is important to know how the collaterals of the lemniscal input fibers are distributed in relation to the curved laminae of the VPL neurons particularly in the absence of inhibitory interneurons in the rat.

The present study describes the cytoarchitecture and dendritic morphology of the VPL neurons and correlates these features with the synaptology of the VPL neuropil. In addition, our investigation of the DCN input to VPL suggests that the collaterals of the input fibers do not conform to the laminar pattern of the VPL neurons but are widespread through the rat VPL.

METHODS

Cytoarchitecture

Standard techniques were used on both frozen and paraffin sections when staining cell bodies with cresyl violet stain. Axons were stained by Bodian's method (Bodian, '36).

Dendritic morphology

Impregnation. Thalami from rats that ranged in age from 21 to 250 days and weighed between 45 and 500 gm were each impregnated by one of two Golgi variations. The largest sample, totaling 22 animals, was processed with the Van der Loos modification of the Golgi-Cox method ('56). The tissue was sectioned at 100 μ m in both the coronal (16 thalami) and horizontal (14 thalami) planes. In the second variation seven animals were sacrificed at 15 or 16 days of age and impregnated by Stensaas' ('67) perfusion modification of the Rapid Golgi method. After this procedure six thalami were cut in the coronal plane and eight in the horizontal plane. Each variation provided a considerable number of well-impregnated neurons, from which could be selected those cells that were the most completely stained and typical of the entire population.

A total of 210 VPL neurons were drawn for analysis but the qualitative features of VPL neurons were supplemented and confirmed by microscopic observation of at least 500 cells. The vast majority of neurons studied were taken from fully mature animals, while the remainder (17 neurons) were selected from

neonatal rats 15–22 days of age. The younger material served only for qualitative comparison, and was not included in any of the quantitative analyses. From the two-dimensional drawings, calibrated measurements were made of (1) the length of proximal dendrites (defined in Results), (2) the total length of each dendrite, and (3) the maximum width of all distal dendritic tufts that arise from a single primary dendrite. Since our objective was only to approximate the extent of the dendritic field, and because a considerable number of dendrites remained parallel to and within the plane of section, no attempts were made to correct the two-dimensional bias.

Ascending afferent fibers

Degeneration studies. Three separate lesion studies were undertaken to assess the thalamic projections from the dorsal column nuclei (comprising both the gracile and cuneate nuclei), the spinal cord, and the deep cerebellar nuclei. Twelve adult rats, weighing between 200 and 450 gm received unilateral dorsal column nuclei (DCN) lesions. Animals were deeply anesthetized with Nembutal (30 mg/kg) or with both Nembutal (21 mg/kg) and Ketamine (60 mg/kg) and their heads were firmly fixed in a stereotaxic apparatus. Large ablations of the DCN were performed using mild suction, which often resulted in a sparing of ventral and rostral portions of the nuclei. Care was taken to avoid damage to the cerebellum or to the tissue underlying the DCN. Radiofrequency heat lesions (20–60 mA for 5–20 seconds) produced damage to smaller portions of individual nuclei. The smallest lesions were produced by a single stab of the gracile nucleus by a wire of 0.02 mm in diameter and were placed in four animals. In an additional three rats a small hole was drilled into the skull and a monopolar tungsten electrode was placed stereotactically into the medial lemniscus at approximately the pontomedullary junction. A radiofrequency heat lesion destroyed the medial lemniscus and some of the surrounding reticular formation.

Four adult rats received high cervical spinal hemisections in an effort to interrupt all spinothalamic and spinocervicothalamic projections. After a dorsal laminectomy of the C2–3 or C3–4 vertebrae, a straight scalpel blade was passed from lateral to medial to the midline. In a few animals, unilateral suction ablations successfully removed one or two spinal segments, but also damaged portions of the contralateral cord.

Finally, ten adult rats received unilateral radiofrequency heat lesions of the deep cerebellar nuclei which damaged approximately half of the deep cerebellar nuclei on any one side. Placement of these lesions was varied from animal to animal to include all of the deep nuclei in some combination.

All lesioned animals were allowed to survive 3–7 days, whereupon they were given an overdose of Nembutal followed by cardiac perfusion of 10% neutral-buffered formalin. Degeneration argyrophilia was plotted on appropriate drawings of sections stained by the method of Fink and Heimer ('67).

Anterograde horseradish peroxidase (HRP) methods. To show the pattern of ascending afferent axons to VPL, 0.2–0.5 µl of 30% HRP was stereotactically placed in the ventral mesencephalon in five rats by slow pressure through a Hamilton syringe with a 26-gauge needle and a Kopf microinjection unit. The syringe needle was placed so that the opening in the beveled face of the needle was directed rostrally. The cutting tip of the needle was passed through the medial lemniscus, cutting many of the ascending afferents. The needle was then raised slightly and the HRP applied to the cut ends of the axons. The large injections were not easily localized but retrograde transport to the DCN and spinal cord confirmed that afferents to VPL from these areas were at least part of the field injected by HRP. Many other brainstem nuclei were also labeled by this procedure. The HRP was visualized by Mesulam's method using tetramethyl benzidine as a chromogen (Mesulam, '78). Some sections were counterstained by neutral red. Drawings were made either under brightfield or darkfield illumination and at a magnification of either $\times 400$ or $\times 1,000$.

EM methods. Samples of VPL were taken from 80 rat brains that had been perfused by cold phosphate-buffered fixative which contained 1% glutaraldehyde and 3% paraformaldehyde. The sample was selected by orienting on the external medullary lamina (Tripp and Wells, '78) and processed for electron microscopy. For quantification of the neuropil, electron micrographs (EM) were taken from the four corners of a grid hole of a 300-mesh grid if the corner was not occupied by a cell body, blood vessel, or group of myelinated fibers. The EM were taken at $\times 6,000$, which did not allow the observer to identify synapses. Fifteen to 30 micrographs from each grid were taken, being careful not to take the same area twice. The area of the neuropil was determined on an en-

larged EM (approximately $\times 18,000$) with the aid of a point lattice. The area of the EM at our standard magnification was determined and the number of points falling on cell bodies, blood vessels, myelinated fibers, and glial processes was subtracted to give the area of the neuropil, and the area of the glial processes. This definition of neuropil differs somewhat from that of Peters et al. ('76) in that all myelinated fibers and glia are excluded. In none of our measurements did we correct for thickness of section. The number of synapses of a certain type were counted in each EM and converted to the number of synapses per $100 \mu\text{m}^2$. The average of the long and short diameters of many of the terminals was determined along with the average diameter of the postsynaptic dendrites. The magnification of the electron microscope was monitored frequently because changes in its operating condition can change the magnification. Thus, we determined the number of synapses of each terminal type per $100 \mu\text{m}^2$, the area of the glial processes, and the average diameter of many of the terminals and their postsynaptic dendrites, combined with our qualitative observations. The method of taking the EM of the sample was biased against axosomatic synapses so they are considered here only qualitatively.

In order to determine the source of the terminal types, large lesions (described previously) were placed in DCN and suction ablations were made in somatosensory cortex. Samples of VPL were removed from 12 hours to 6 days after the lesion and analyzed as above. In order to correlate the size of the lesion in DCN with the degree of degeneration in VPL, the area of viable neurons in serial sections was determined by planimetry on both the lesioned and unlesioned side. The percentage difference was taken as the percentage of DCN that was damaged by the lesion.

The animals used in all of the above experiments were Sprague-Dawley rats.

RESULTS

The ventrobasal complex (VB) of the rat thalamus consists of two nuclear subdivisions, a ventral posterolateral nucleus (VPL) and a ventral posteromedial nucleus (VPM). Other authors have identified the lateral subdivision as the pars externa or lateralis and the medial subdivision as the pars arcuata, interna or medialis, of VB (Lund and Webster, '67a,b; Jones and Leavitt, '74). Since the present report focuses specifically on VPL, careful cytoarchitectural delineation of this particular subdivision

is required at the outset. VPL comprises the most external portion of VB (Fig. 1), and is bordered laterally by the external medullary lamina (EML) and medially by VPM. This demarcation is especially prominent along the middle of the rostrocaudal extent of the nucleus, and throughout the entire dorso-ventral extent of VPL. Rostral and caudal poles of VPL, however, are more difficult to delineate, because VPL neurons blend with those of adjacent regions, namely, ventral lateral nucleus (VL) rostrally and posterior thalamic complex (PO) caudally.

On the basis of cytoarchitectural features, connectivity, and dendritic morphology, the present study demonstrates that VPL curves medially to partially cover the rostral pole of VPM and ends 700–1,000 μm from the extreme rostral limit of the thalamic ventral tier nuclei. A transition zone, composed of neurons with cytological and dendritic features common to both VL and VPL, is found at the rostral pole of VPL (Fig. 2). Our degeneration studies suggest that at least part of this region receives overlapping inputs from spinothalamic neurons, DCN, lateral cervical nuclei, and deep cerebel-

Abbreviations

AC	anterior commissure
Am	anteromedial nucleus
AP	anterior preoptic area
Av	anteroventral nucleus
C	cuneate nucleus
CL	central lateral nucleus
CM	central medial nucleus
CM-Pf	centromedian-parafascicular complex
ctz	caudal transition zone
DM	dorsomedial nucleus
F	fornix
FC	fasciculus cuneatus
FR	fasciculus retroflexus
G	gracile nucleus
IC	internal capsule
LGN	lateral geniculate nucleus
LGv	lateral geniculate nucleus pars ventralis
MG	medial geniculate nucleus
ML	medial lemniscus
NS	solitary nucleus
PO	posterior thalamic complex
PO1	lateral part of posterior thalamic complex
POm	medial part of posterior thalamic complex
Pv	paraventricular nucleus
R	reticular nucleus
rtz	rostral transition zone
SN	substantia nigra
SpV	spinal trigeminal nucleus
VL	ventral lateral nucleus
VM	ventral medial nucleus
VPL	ventral posterolateral nucleus
VPM	ventral posteromedial nucleus
ZI	zona incerta
IV	fourth ventricle

lar nuclei, and correspond to a transitional area between VL and VB in the cat described by Strick ('73) and Jones and Burton ('74). Similarly, the caudal pole of VPL appears to be limited by the fibers of the EML that curve medially to form a cap around the entire thalamic ventral tier nuclear complex, and, in so doing, separate the pretectal region from the dorsal thalamus (Scalia, '72). Cytoarchitectural differences are apparent as VPL merges with lateral portions of PO so that a second transition zone is associated with VPL, located in this instance at the caudal boundary of the nucleus (Fig. 2).

Cytoarchitecture

The neurons that populate VPL consist of multipolar discoid cells. The coronal and horizontal planes have medium-sized, oblong, or fusiform somata with their long axes predominantly oriented parallel to the EML. These neurons present a striking appearance of a series of concentric cellular laminae that course rostrocaudally and dorsoventrally

throughout the nucleus (Fig. 2). The laminar pattern is distorted in ventrolateral portions of VPL only by thalamic radiation fibers which displace adjacent neurons.

At the extreme rostral pole of VPL, the discoid somata so characteristic of more intermediate portions of VPL turn medially away from the EML to form a partial cap over the rostral-lateral aspect of VPM (Fig. 2).

The rostral pole of VPL occupies progressively more caudal levels as its ventral border is approached. The rostral transition zone is located adjacent to the medial curvature of VPL, along the lateral border of the area that is usually regarded as the VL nucleus (Faull and Carmen, '78). It is often difficult to identify the rostral transition zone purely on cytoarchitectural grounds, but it appears to consist of discoid neurons that continue rostrally from VPL into lateral portions of VL (Fig. 2), where it is mixed with rounder and larger cells.

The caudal transition zone is characterized by neuronal somata that are much less discoid than the neurons typically found in VPL, and

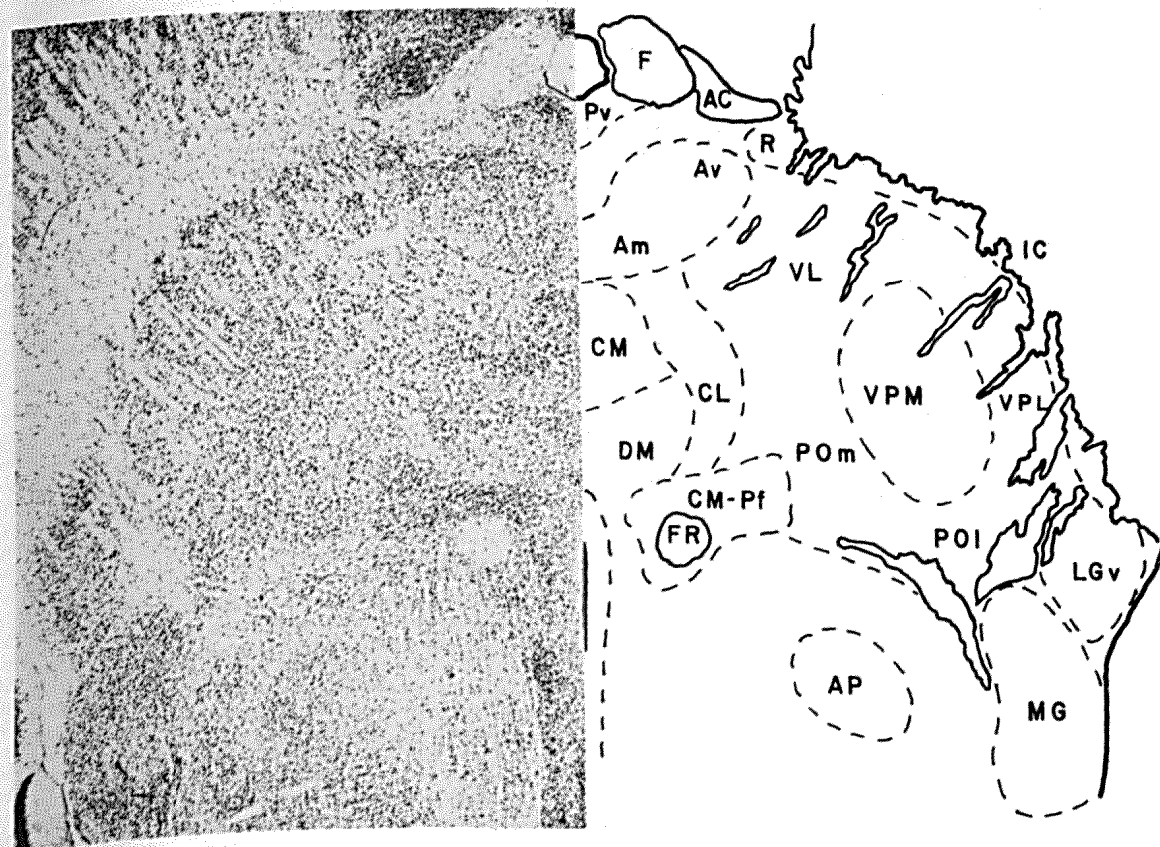


Fig. 1. Horizontal view of the rat thalamus. The diagram on the right indicates the position of the nuclei that are present in the cresyl violet-stained section on the left. The horizontal plane offers the most comprehensive view of the VPL and is used in most of the subsequent illustrations.

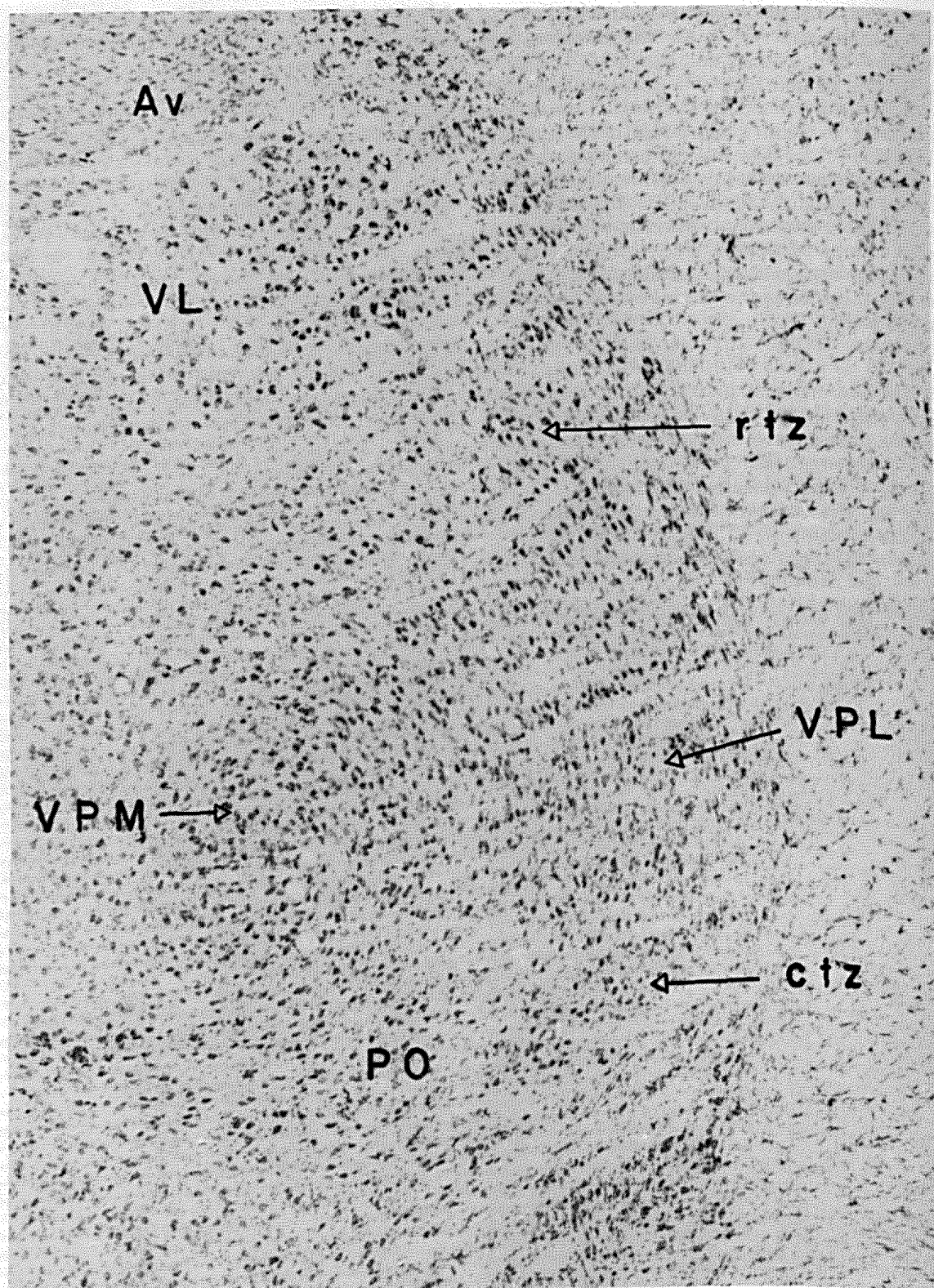


Fig. 2. Horizontal section through the ventral tier nuclei. VPL is bounded rostrally by a zone that is transitional with VL (rtz) and caudally with a zone that is transitional with PO (ctz). VPL neurons form rows of cells that start parallel to the external medullary lamina on the right of the photomicrograph and describe segments of concentric circles of decreasing radii that are centered in VPM. Cresyl violet stain. Magnification $\times 256$.

exhibit no apparent laminar orientation (Fig. 2). Smaller somata become more prevalent as the caudal border of VPL is approached, and since these cells are nearly identical to those that homogeneously populate the posterior thalamic complex, it appears that the caudal transition zone represents an overlap of VPL and PO.

Dendritic morphology

The cytological features of VPL neurons observed in Nissl preparations are also apparent in Golgi impregnations. The nucleus is composed exclusively of medium-sized, multipolar neurons whose somata are predominantly fusiform in the coronal and horizontal planes, depending somewhat on the region of VPL examined. Neurons that populate the entire lateral border and most of the rostral two-thirds of VPL have somata that are markedly flattened (Figs. 2 and 3). The lateral neurons also conform best to a laminar pattern and can be seen to be aligned in rows along with their dendrites (Fig. 3).

The surfaces of all VPL neuronal cell bodies are quite smooth, and no somatic appendages are apparent. Relatively thick primary dendrites, numbering from two to seven but averaging 4.3 per cell, emanate from each soma (Fig. 4). The mean length of these dendrites, calculated from 236 such branches measured from both coronal and horizontal sections, is $24.5 \mu\text{m}$, but a wide range between 4 and $85 \mu\text{m}$ exists. This broad range most likely reflects the fact that the length measurements were taken from two-dimensional projection drawings, and thus primary dendrites which angle sharply away from their point of origin would appear much shorter than their real length.

Short, blunt appendages on primary dendrites are seen following the Stensaas impregnation procedure but rarely after Golgi-Cox impregnation. A characteristic feature of thick primary dendrites is that they extend, without tapering, to a point where they abruptly give rise to a cluster of secondary (or tertiary) branches whose diameter is quite thin. We refer to this branching pattern as a "whorl" and use it as one of the main criteria for determining the termination of this type of primary dendrite (Fig. 5). Occasionally the thick primary dendrites may subdivide and give rise to two or three secondary branches, each having the same morphology as the original stem dendrite (Fig. 4). Such secondary branches remain quite thick and usually terminate in a whorl of thin tertiary branches (Figs. 5A-C;6). Based on

three criteria—increased thickness, presence of sparse blunt appendages, and termination as a whorl of secondary or tertiary branches, we have referred to these stem dendrites as *proximal dendrites*. Thus, by definition, proximal dendrites are most often primary branches, but thick secondary dendrites are included in this category occasionally. The proximal dendrites were often aligned in parallel to the curved laminae of VPL (Figs. 3 and 4) although a few proximal branches crossed the lamina (Fig. 4).

In rare instances, a thin dendrite with no appendages and few subsequent branches can be seen emanating from either the proximal dendrite or directly from the soma. Although the whorl pattern of branching is a common feature of rat VPL neurons, one variation of this branching pattern does exist. The grouping of secondary or tertiary dendrites may also result from a succession of branches arising from the same small area of a proximal dendrite (Fig. 5B,D). Similar to the whorl pattern, these distal dendrites arise at the end of the thick proximal stump, and their diameters are markedly reduced. Such thin secondary or tertiary branches, which emanate either as a whorl or a tuft from a thick proximal dendrite, have been termed *distal dendrites*. Thus, the terms *proximal dendrite* and *distal dendrite*, as defined herein, will be used throughout this report to describe the dendritic morphology of VPL neurons.

Distal dendrites can give rise to one or two long unbranched tertiary or quaternary dendrites, but multiple branch points and greater than fifth-order dendrites are seldom observed (Figs. 5 and 6). While these distal dendrites do radiate from common or close branch points on or near the end of the proximal dendrite, they usually course in close proximity to each other (Figs. 5, 6). Thus, they form a sheaf of distal dendrites resembling an inverted cone, with the apex of the cone represented by the origin from the proximal dendrite. Distal sheaves arising from a single proximal dendrite, and consisting of two to four unbranched distal dendrites, will encompass a maximum width of approximately $120 \mu\text{m}$. A single proximal dendrite which emits two or three thick branches, each of which gives rise to a large sheaf with many branches, usually produces a large dendritic field that may radiate a full 180 degrees (Fig. 5C) from the parent soma. Termination of distal dendrites occurs between 70 and $230 \mu\text{m}$ from the soma, but the shorter lengths can be misleading. It is possible that these figures represent dendrites that were cut off as they

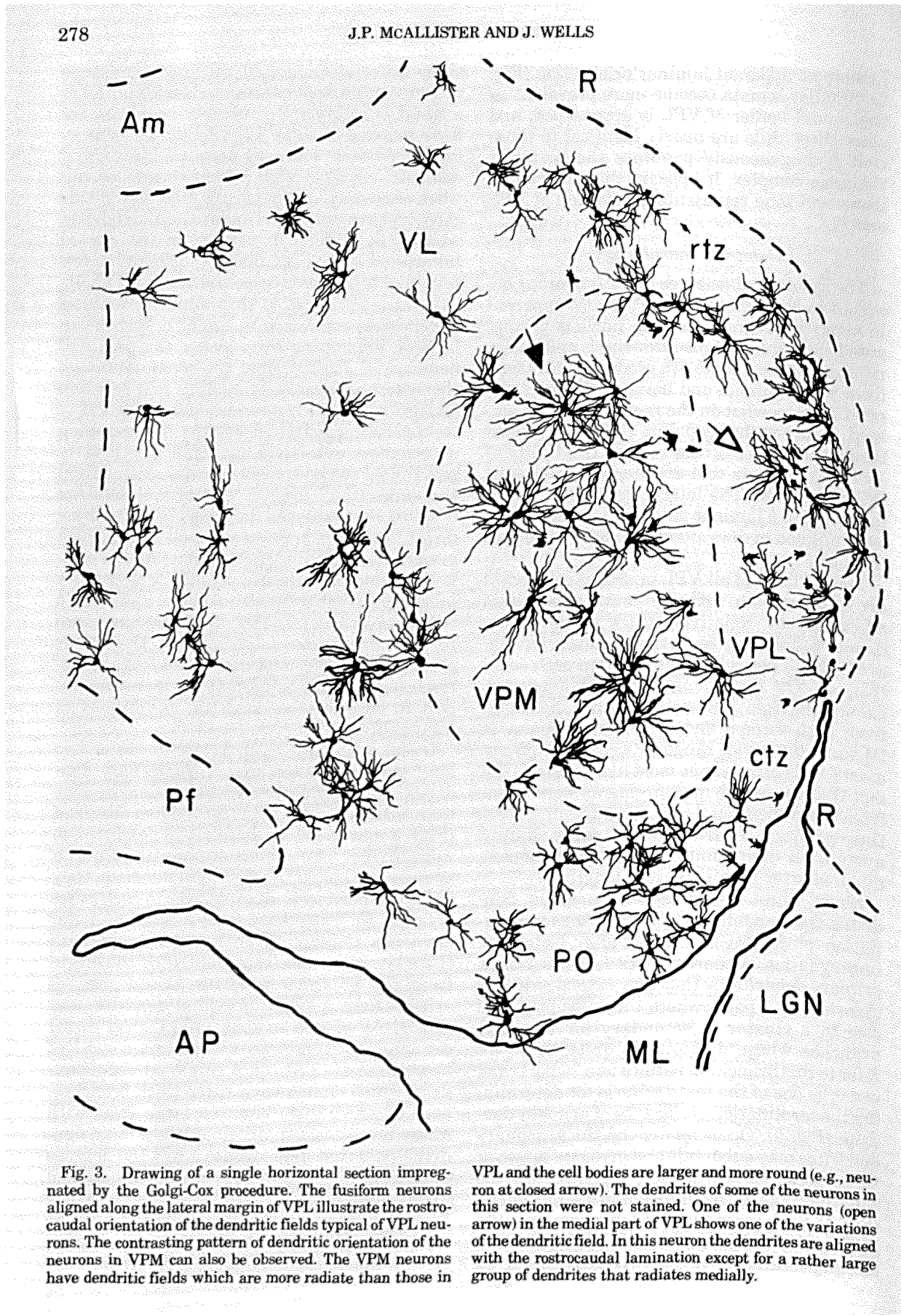


Fig. 3. Drawing of a single horizontal section impregnated by the Golgi-Cox procedure. The fusiform neurons aligned along the lateral margin of VPL illustrate the rostro-caudal orientation of the dendritic fields typical of VPL neurons. The contrasting pattern of dendritic orientation of the neurons in VPM can also be observed. The VPM neurons have dendritic fields which are more radiate than those in

VPL and the cell bodies are larger and more round (e.g., neuron at closed arrow). The dendrites of some of the neurons in this section were not stained. One of the neurons (open arrow) in the medial part of VPL shows one of the variations of the dendritic field. In this neuron the dendrites are aligned with the rostrocaudal lamination except for a rather large group of dendrites that radiates medially.

passed out of the 100- μm -thick section, but this is unlikely, since care was taken not to measure any branches that appeared truncated or not impregnated completely. Therefore, the longer lengths are better estimates of the actual length of the distal dendrites.

The distal dendrites have small varicosities and short appendages along the entire length of the dendrite (Figs. 5 and 6). The varicosities occur about every 5 to 10 μm along each branch. Appendages are relatively sparse on distal dendrites, and appear either as spines with a thin neck and enlarged head, or most often as simple thin shafts extending 1–2 μm from the surface of the dendrite. In addition, long thin

shafts can often be seen selectively in contact with the varicosities of distal dendrites, and may easily be confused with a form of dendritic appendage (Figs. 5B, 6A). Closer examination reveals, however, that these appendages are in fact broken preterminal axonal branches, because in fortuitous sections, these processes can be traced for some distance from the point of dendritic contact to beyond the limits of that particular dendritic field. They always remain thin throughout their length, possess rather large varicosities, and are completely devoid of appendages. Furthermore, they can give rise to collateral branches, and exhibit grapelike clusters (Fig. 6A) which Tömböl ('66/67, '69a) has

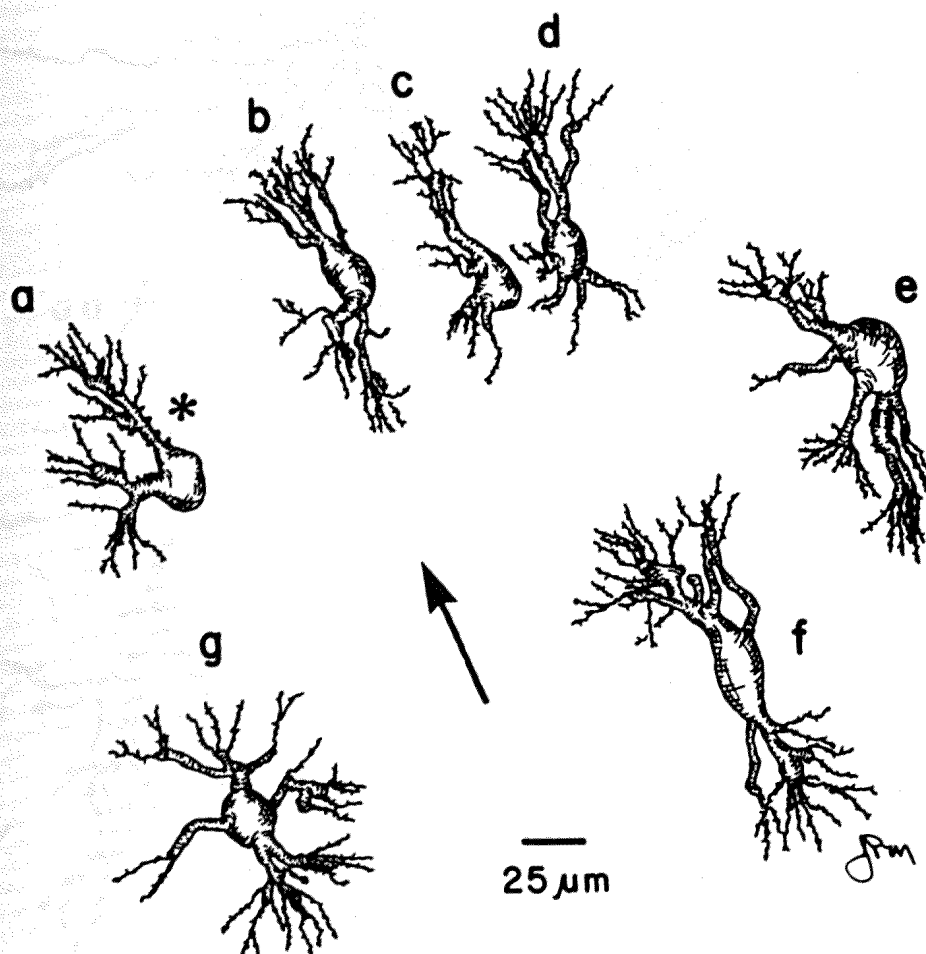


Fig. 4. Drawings of Golgi-impregnated neurons from VPL showing the morphology of proximal dendrites. Only the cell bodies, proximal dendrites, and initial portions of the distal dendrites were drawn in this figure. The arrow points rostrally and indicates the direction of the laminae relative to each neuron. Lateral VPL is to the right of each soma. The proximal dendrites have short blunt dendritic appendages (a,*) and are uniform in diameter until they branch into distal dendrites. Neurons b, c, and d were drawn as viewed in

the same section, as were neurons e, f, and g from a different section. These two groups illustrate that neurons in close proximity can have varying branching patterns. Neuron f has all proximal dendrites aligned with the laminae including one that leaves the lateral aspect of the soma and bends to conform to the laminae. Neuron g has proximal dendrites which radiate in all directions from the soma. Very few cells had proximal dendrites that were directed laterally. Stensaas procedure. Horizontal sections.

previously identified as terminal axonal arborizations. The pattern of dendrites which are most typical of VPL is found in Figure 6.

Dendritic orientation. The most conspicuous feature of the dendritic morphology of VPL is the orientation of proximal and distal branches. In general, VPL contains neurons with flattened dendritic fields oriented parallel to the EML, giving the nucleus a laminated appearance. As previously noted, the majority of neurons found in VPL have discoid somata, with a long diameter approximately twice the length of the short diameter. Golgi impreg-

nations of these cells, viewed in the horizontal plane, show that nearly 66% of all proximal dendrites project from either the rostral or caudal poles of each soma and remain parallel to the EML. Among the other dendrites, it was not uncommon to observe medially and laterally directed proximal branches, especially in more medial portions of VPL (Fig. 3). Often these stem dendrites, after extending 20 to 30 μm from the soma, give rise to distal dendrites that bend and course in either a rostral or caudal direction (Fig. 5). The dendritic trees formed from a single proximal dendrite usually expand

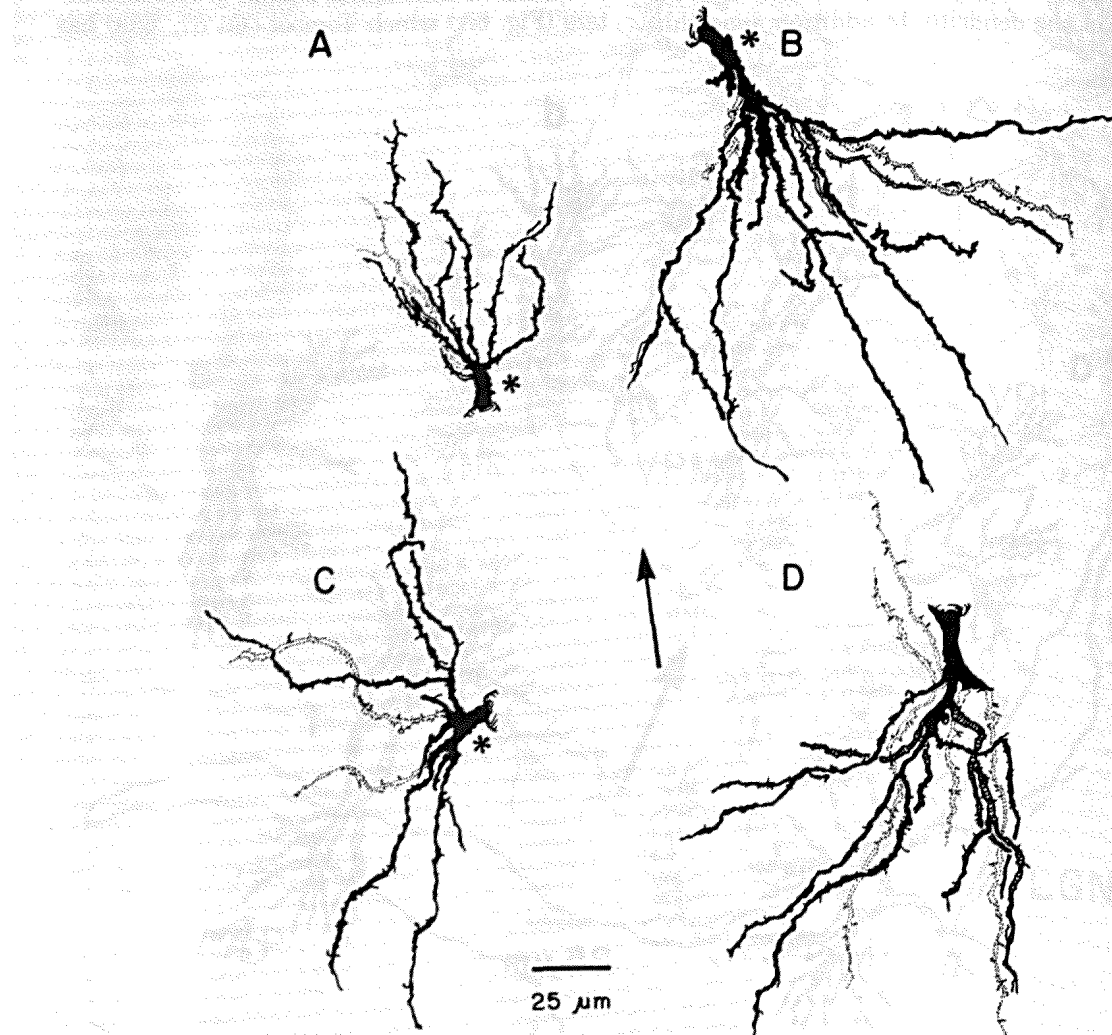


Fig. 5. Drawings of Golgi-impregnated dendrites of VPL neurons showing the branching pattern and orientation of the distal dendrites. The arrow is pointing rostrally in A, B, and D, which are from horizontal sections, and dorsally in C, which is from a coronal section. Lateral is to the right in A-D. Open, stippled, and hatched branches refer to dendrites that course beneath the blackened branches. Spines can be seen on the distal dendrites as well as short blunt appendages on

proximal dendrites (*), but both are relatively infrequent. A. The typical whorl pattern of the distal dendrites. B. The distal dendrites originate from the proximal denrite in a successive branching pattern. C. The distal dendrites from one proximal dendrite radiate over 180°. D. Distal dendrites are often grouped together rather than fanned out. Stensaas procedure. Drawings made at $\times 1,000$.

to about 120 μm at a distance of 170–230 μm from the point of origin on the soma surface. In the event that a single proximal denrite gives rise to two or three thick secondary branches, each of which produces an extensive sheaf of distal dendrites, the dendritic field which results may radiate up to 180 degrees from its origin and cover up to 275 μm in width (Fig. 5C). Thus, the overall shape of the dendritic field depends on the number of proximal den-

drites emanating from a particular neuron, their point of origin and orientation, and the number of times they branch before giving rise to a sheaf distal dendrites.

Although Golgi-impregnated material sectioned either in the sagittal plane or tangential to VPL (parallel to the EML) has not been examined, it appears by extrapolation from the horizontal and coronal planes that most neurons that populate VPL have dendritic domains

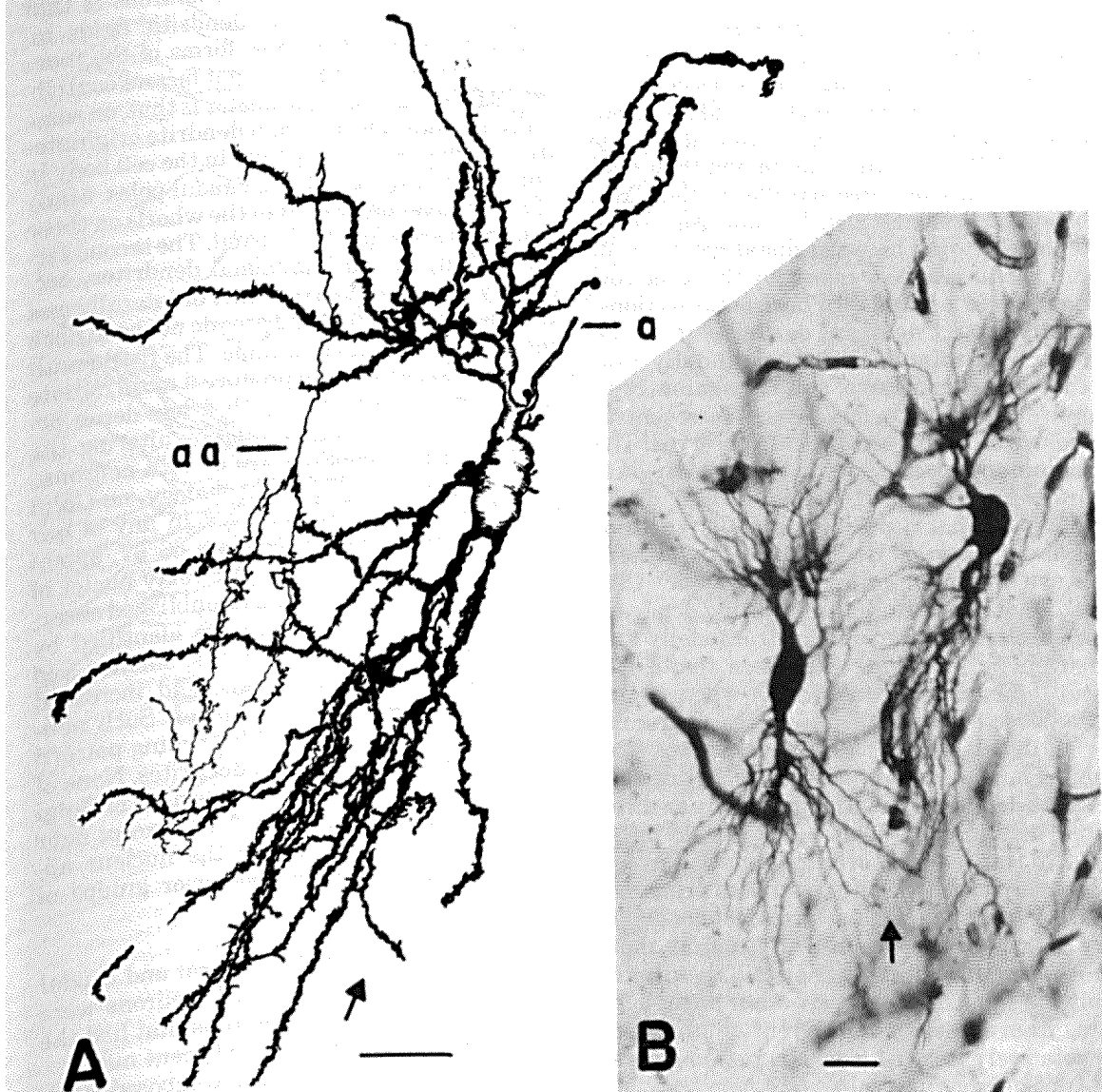


Fig. 6. Typical neurons of VPL. A. Drawing of a typical VPL neuron done at $\times 1,000$, stained by the Golgi-Cox procedure. The whorl pattern can be seen in the distal dendrites. The proximal dendrites conform to the lamina orientation of the VPL neurons. Some of the distal dendrites are aligned with laminae and some fan out across laminae. The caudally directed distal dendrites in A are grouped into sheaves.

a: The axon of the VPL neuron; aa: an axon from an unknown source passing through the dendritic field of the VPL neuron. B. Photomicrograph of two typical VPL neurons stained by the Stensaas procedure. Both the whorl pattern and the dendritic sheaves can be observed. In both A and B the closed arrow points rostrally along a lamina in these horizontal sections with lateral to the right. Bar, 50 μm .

shaped like a biconcave disc with the soma at its center. The dendritic domains are oriented parallel to the curvature of the EML, and contain three to seven dendrites (Figs. 4 and 6). In both horizontal and coronal sections neurons with biconcave disc-shaped dendritic domains are most often located closer to the EML. On rare occasions, lateral dendrites can be observed mingling with fibers and dendrites or medial portions of the thalamic reticular nucleus.

Lamination and overlap of dendritic fields. It is important to note the structural relationship between the arrangement of discoid somata organized into concentric lamellae, and the orientation and overlap of individual dendritic fields. In VPL, both the somata and their dendritic fields are oriented parallel to the EML. Whole field drawings clearly show (Fig. 3) the extensive overlap between distal dendrites of neurons which appear to occupy the same row of neurons in a lamina. In horizontal sections, rostrally projecting distal dendrites from one neuron intermingle with the caudally projecting distal dendrites of another neuron. Similar overlap is apparent in the dorsoventral plane when coronal sections are observed. The predominant discoid character of individual neurons promotes such overlap. Indeed, whole field views that contain numerous well-imregnated neurons demonstrate that these cells are organized in linear arrays, such that rows of neurons with interdigitating dendritic fields are formed that run rostrocaudally and dorsoventrally within VPL. Less frequently distal dendritic overlap results when a medially directed dendrite crosses the rostrocaudal or dorsoventral rows of dendrites. Extremely long medial (or lateral) dendrites may cross the dendritic domains of as many as three to ten neurons and span a distance of up to 250–275 μm from the original neuron.

The extensive overlap is restricted primarily to distal dendrites because proximal dendrites only extend an average of 24.5 μm from their parent soma. Proximal dendrites, then, cohabit the same area as many other distal dendrites from a variety of different neurons, yet are relatively isolated from the proximal dendrites of neighboring cells.

Variations in the basic pattern. Throughout VPL, neurons are occasionally found whose branching patterns and dendritic orientations differ from the predominant type described above. Some of these dendrites are thick and smooth-surfaced, but they do not end abruptly,

nor do they give rise to a whorl or cluster of distal dendrites, although they do end in successive alternate branches. Nevertheless, it is usually possible to determine a point along the dendrite at which the diameter changes markedly and more distal branches arise. That junction is considered the termination of the proximal dendrite. Usually, proximal dendrites which branch in this fashion end approximately 30 to 45 μm from the soma.

A second variation of VPL neurons is that they may exhibit radiate dendritic fields instead of the biconcave disc forms of the more typical neurons. Two principal factors contribute to this variation. One factor is that, on some VPL neurons, the proximal dendrite originates from medial or lateral points in the cell body in addition to the rostral and caudal poles. Many of the sheaves derived from the whorls on these dendrites are wider than usual. The second factor is that, in some proximal dendrites, secondary branches turn medially or laterally and the sheaves of distal dendrites do not bend back into the rostrocaudal laminae. The final result of these variations is to produce a more radiate field of distal dendrites with a less dense accumulation of branches, thereby altering the characteristic tufted pattern of VPL neurons.

Based upon dendritic morphology, no Golgi type II neurons were observed in any of our preparations. In the cat (Tömböl, '66/'67, '69a,b) and in other specific thalamic relay nuclei of the rat (Lieberman, '73 and unpublished observations) intrinsic neurons were identified by their sparse branching patterns, smaller and more radiate dendritic fields, and increased numbers of dendritic appendages. Such neurons never exhibit a whorl branching pattern that forms sheaves of distal dendrites. None of these dendritic features characteristic of Golgi II neurons were observed in VPL, except near the caudal boundary where the nucleus appears to blend with the posterior groups of thalamic nuclei.

Transition zones. At the rostral and caudal poles of VPL, the typical VPL neurons were observed to mingle with neurons that had the structural characteristics of adjacent nuclei.

The rostral transition zone is composed of two kinds of cells (Fig. 7). Some had discoid cell bodies, thick proximal dendrites, and a sheaf of distal dendrites originating from a whorl, i.e., typical VPL neurons (Fig. 7A,C). The second kind of neuron was characteristic of VL. Neurons in VL are characterized by large round cell bodies with radiate dendritic fields (Fig. 7B).

Distal dendrites of the VL cells are moderately branched, originate from thick proximal dendrites, but do not form a whorl. The discoid cells are most prominent in the lateral margin of the transition zone, and it is in this lateral region where there is overlapping input from DCN, spinal cord, and cerebellum (see below).

The caudal transition zone is found in the caudal and medial region of VPL (Fig. 3). The

typical discoid VPL neurons are present but are no longer strictly aligned parallel to the external medullary lamina (EML) in conformation with the laminar pattern. The fusiform cells appear more randomly oriented. Because of the loss of lamination, there is considerably more overlap with the dendritic domains of other neurons. The dimensions of the dendritic fields in the discoid cells are similar to those in the

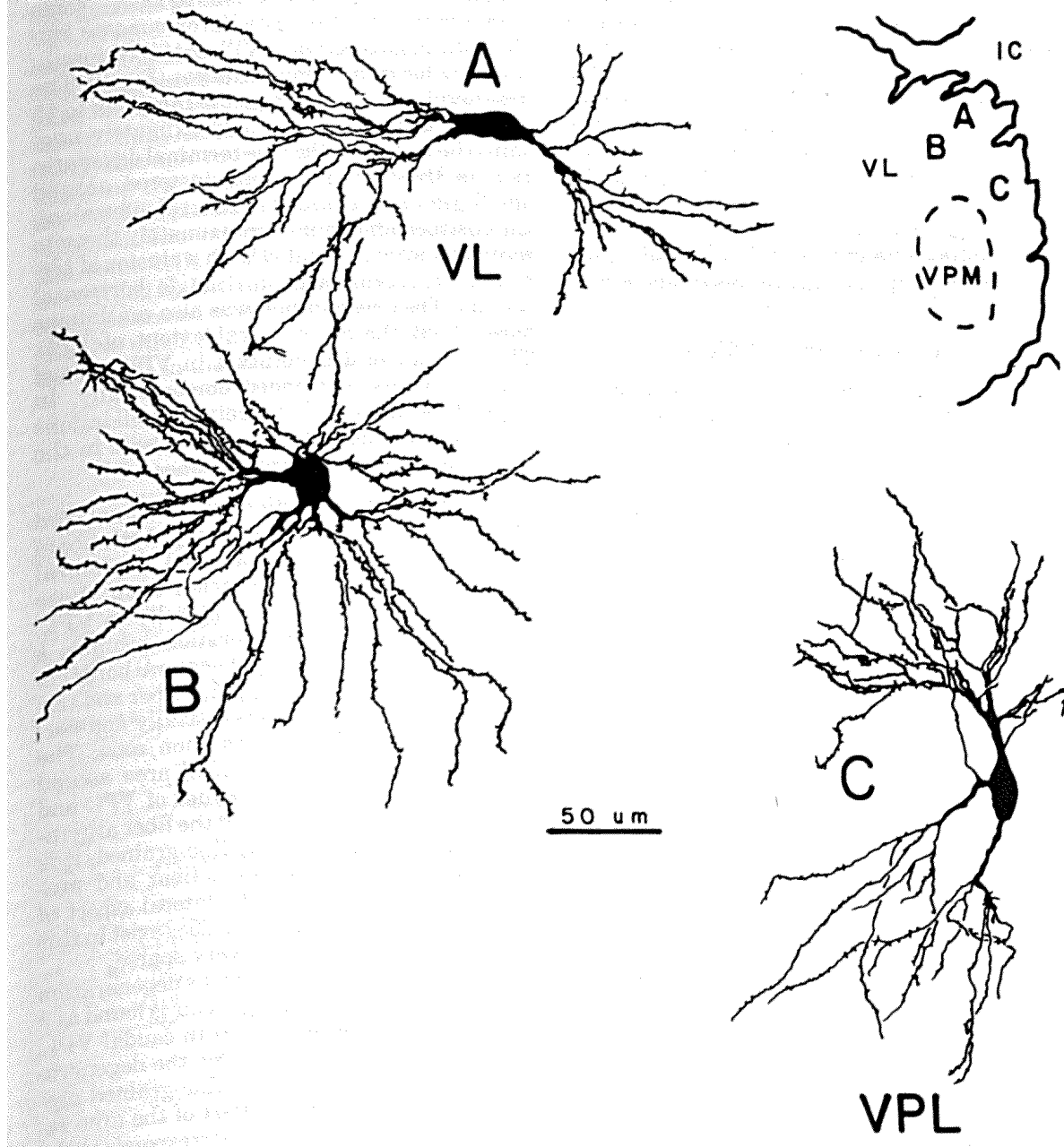


Fig. 7. Drawings of neurons found at A, B, and C on the VPL. B. A neuron with the characteristics of a VL neuron also located in the rostral transition zone. C. A neuron from VPL that shows the common features of a typical VPL neuron. Drawings made at $\times 400$. Horizontal section.

VPL. B. A neuron with the characteristics of a VL neuron also located in the rostral transition zone. C. A neuron from VPL that shows the common features of a typical VPL neuron. Drawings made at $\times 400$. Horizontal section.

laminated region of VPL. The appearance of the caudal transition zone is further complicated by the presence of neurons that have the characteristic structure of PO neurons. The boundary between PO and VPL is difficult to delineate precisely (as in the cat, Jones and Burton, '74) but PO neurons have a dendritic morphology sufficiently different from VPL neurons such that distinctions can be made. In general, PO neurons have primary dendrites of varying diameter, often quite thin in caliber with no basal thickening, smaller radiate dendritic fields with less frequent distal dendrite branching and increased numbers of dendritic spines, compared to adjacent VPL neurons. The whorl type of branching pattern is rarely observed in PO neurons, and both PO and caudal VPL neurons exhibit an alternate branching of their distal dendrites.

Ascending afferents from DCN and spinal cord also overlap laterally in this caudal region (see below).

Ascending afferent fibers

Lund and Webster ('67a,b) have previously described the major ascending projections to VPL using degeneration methods. We have repeated these experiments in order to more clearly define the rostral and caudal transition zones. We also have made small lesions in DCN to correlate lemniscal input with the apparent lamination of the VPL neurons. In addition we have injected HRP into the mesencephalon to determine the pattern of distribution of afferent axons in VPL. All of the ascending afferent fibers to VPL also project to other areas but we shall not comment on those projections.

Dorsal column nuclei. While none of our lesions completely destroyed DCN, the case shown in Figure 8 represents the most extensive damage to DCN without concomitant involvement of adjacent brainstem structures. This lesion, in which only extreme rostral and extreme caudal extensions of the nuclei were spared, produced degeneration argyrophilia throughout the entire contralateral VPL. Degenerating fibers are characteristically large and, within VPL, course mainly in a rostrocaudal direction parallel to the EML. In this case terminal degeneration is quite dense and can be observed throughout the nucleus except in small areas along the medial border and within the caudal pole of VPL. The vacant areas are probably related to the unlesioned part of DCN because large lesions of the ipsilateral medial lemniscus at midbrain levels produce degen-

eration which fills these vacant areas. Both fiber and terminal degeneration appear to extend into the rostral transition zone. The DCN input into the rostral transition zone is especially prominent within the dorsal part of VPL, and is a consistent feature of the DCN projection. No projections from DCN or from the medial lemniscus extend rostrally to the reticular thalamic nucleus.

Following very small lesions of DCN—some single stabs of either gracile or cuneate nuclei—the degeneration in VPL extended rostrocaudally for rather long distances (Fig. 9). The degeneration was sparse and spanned ten to 15 rows of VPL neurons or approximately one-third the width of VPL. The terminal degeneration in these animals was clustered around small groups of neurons at several sites along the rostrocaudal path. Approximately three to four cells were associated with a cluster of terminal degeneration in any single horizontal section. The degeneration was also continuous throughout the dorsoventral extent of VPL. The corridor of degeneration in VPL started ventrocaudally and ended dorsorostrally. In some of the animals that received small lesions a few degenerated fibers could be seen in the rostral and caudal transition zones.

Spinal cord. Hemisections of the spinal cord at cervical segments 2–4 interrupt both fibers from the spinothalamic tract and the lateral cervical nucleus. Degeneration from those hemisections is produced bilaterally in VPL. Ipsilateral terminal degeneration occupies a crescent-shaped area along the lateral border of the rostral VPL (Fig. 10). Sparse fiber and terminal degeneration spreads rostrally and dorsally into the VPL-VL transition zone. The axons which supply this rostral area ascend along the extreme lateral border of VPL and because both the terminal and the fiber argyrophilia are characteristically fine-grained, it is often difficult to distinguish fiber and pre-terminal degeneration in the lateral aspect of VPL. If terminal degeneration does exist in this lateral region of VPL, it is very sparse.

The second area of conspicuous degeneration of the ipsilateral spinal projections is found as a region of sparse degeneration in caudal VPL. Like the rostral transition zone the degeneration in this caudal region is fine-grained pre-terminals and thin fibers. Part of the area receiving the spinal projection corresponds to the caudal transition zone between VPL and PO.

Cerebellum. Lesions of the deep cerebellar nuclei confirmed the projections from the cere-

bellum that were observed by Faull and Carmen ('78). This projection passes medial to the ventrobasal complex to reach PO, VL, and the rostral transition zone. Preterminal degeneration was observed in the medial part of the posterior thalamic complex.

Antegrade HRP. Injections of HRP into the ventral mesencephalon allowed us to observe the general pattern of ascending afferents in VPL (Fig. 11). The injection site was not well localized to a specific tract and inferential evidence suggested that many major thalamic inputs were involved, not just the lemniscal input. Many cells of the cerebral cortex were filled through retrograde transport of HRP, implying the descending cortical pathways of the cerebral peduncle also were involved in the injection. The anterior nuclei of the thalamus and some cells in the lateral group of nuclei were filled by HRP and the axons of these cells could be traced to the mesencephalic injection site. No other thalamic neurons were filled so that axons in the thalamus which could not be

traced to the thalamocortical bundles or to the anterior and lateral nuclei were presumed to be axons of ascending thalamic afferents which passed through the effective injection site and transported the HRP in the antegrade direction.

Two distinct patterns of ascending afferent fibers were observed in horizontal sections (Fig. 11). One group of afferent fibers entered the thalamus caudally, passed along the medial side of VPM, and distributed fibers to the midline, intralaminar, posterior, and VL nuclei with some fibers crossing in a thalamic decussation. As this pathway progressed rostrally, it curved laterally around the rostral margin of VPL and VPM and occupied the full extent of VL. The medial pathway consisted of very thin fibers that formed a network of axons without a predominant directional orientation. The second group of afferents entered the thalamus caudally and ventrally and passed along the lateral side of VPM and distributed afferents to the posterior nuclei and VPL. VPM itself received afferents from the laterally directed fi-

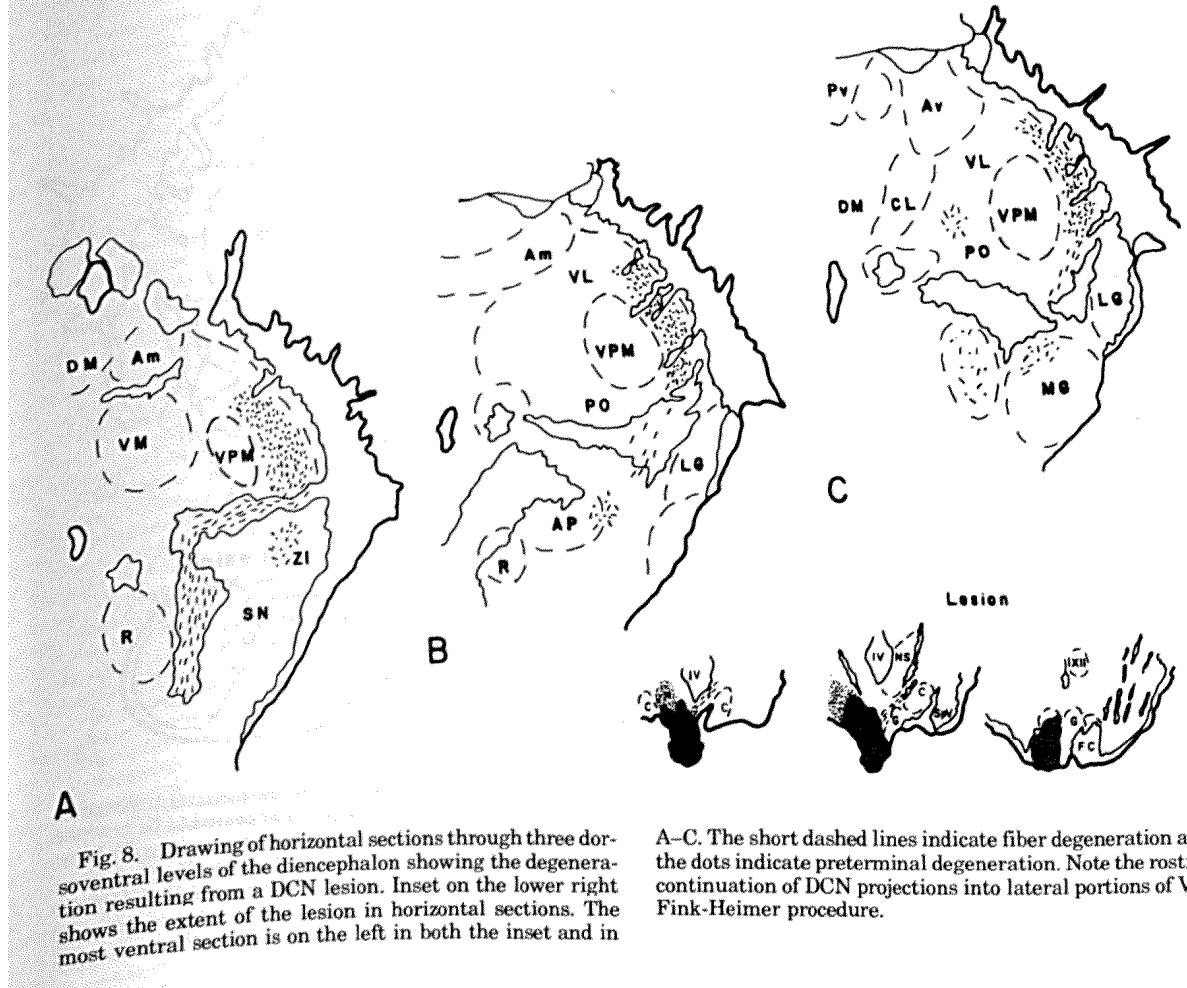


Fig. 8. Drawing of horizontal sections through three dorsoventral levels of the diencephalon showing the degeneration resulting from a DCN lesion. Inset on the lower right shows the extent of the lesion in horizontal sections. The most ventral section is on the left in both the inset and in

A-C. The short dashed lines indicate fiber degeneration and the dots indicate preterminal degeneration. Note the rostral continuation of DCN projections into lateral portions of VL. Fink-Heimer procedure.

bers although in Figure 11 the trigeminothalamic fibers were not filled by HRP and VPM contains few axons. The two patterns suggest that the major medial pathway derives from the dentato-rubro-thalamic pathway (Faull and Carmen, '78) and the major lateral pathway derives from the medial lemniscus. The degree to which these ascending pathways were labeled by HRP varied from animal to animal. In some animals only the lateral projection was filled by the HRP and in others only the medial pathway was filled. The proportion of each pathway which was filled also varied among animals. The course through the thalamus of individual fibers could be observed best when relatively few fibers were labeled. When the pathway was more completely labeled, the pattern of small-diameter afferent axons could be observed best. We emphasize below the pattern observed in the lateral pathway which brings ascending fibers to VPL.

Retrograde transport of HRP to the dorsal column nuclei (Fig. 12), trigeminal nuclei, spinal cord, reticular formation, and deep cerebellar nuclei implied that pathways emanating from these areas were also filled in the anterograde direction by the injection in the ventral mesencephalon. Most of the axons to VPL, however, were probably from the DCN because, when the DCN were lesioned prior to the injection of HRP, no HRP-filled axons were seen in VPL, although they were observed in VPM (Fig. 13).

The lateral afferent supply to VPL enters the thalamus caudally and ventrally and in general courses through VPL in roughly parallel rows that conform to the curvature of VPL. The general pattern of the large-diameter axons tends to reinforce the laminated appearance of VPL but many of the smaller-diameter fibers did not conform to the pattern of parallel arrays. Many of the larger-diameter fibers could be seen to course for long rostrocaudal dis-

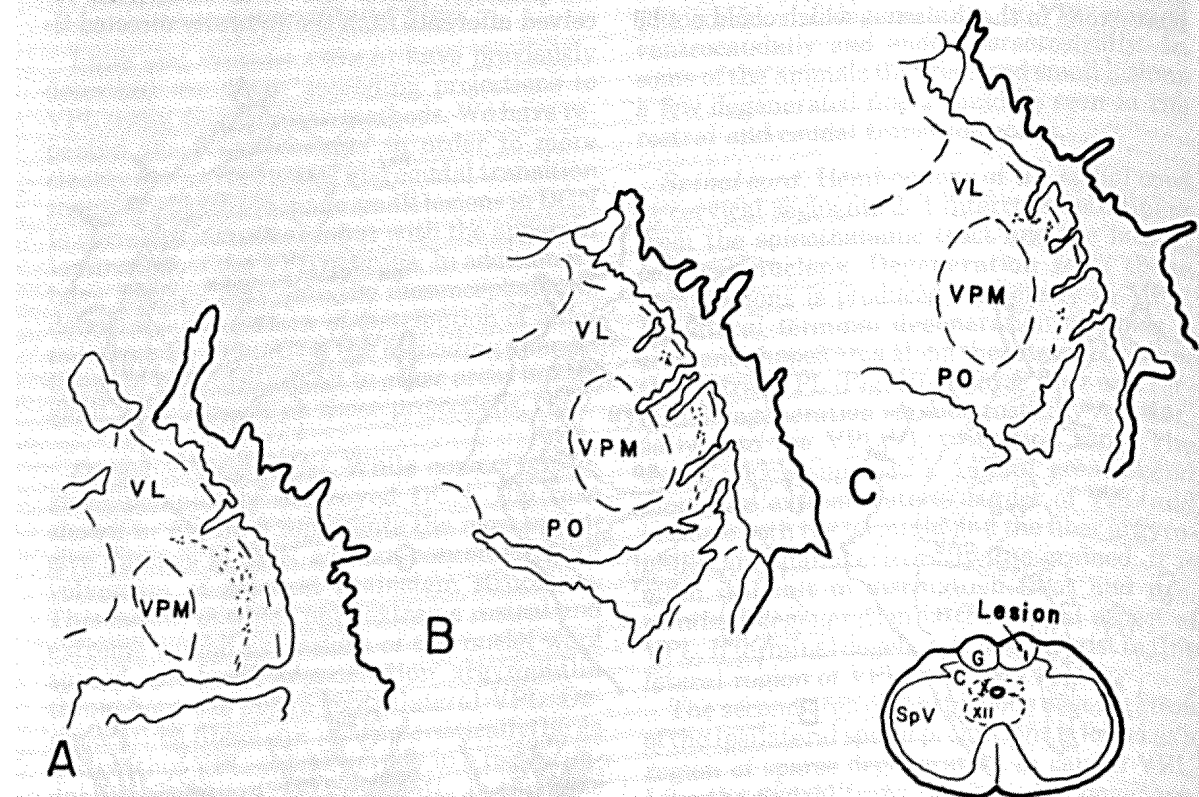


Fig. 9. Drawing of horizontal sections through three dorsoventral levels of the thalamus showing the degeneration in VPL resulting from a single stab lesion of the DCN. The inset on the lower right shows the location and relative size of the lesion in a coronal section of the medulla. The lesion was 60 μm wide. The band of degeneration in VPL extends throughout the rostrocaudal extent of the nucleus and has a wide

mediolateral spread particularly in the more ventral section (A). The preterminal degeneration appeared to be grouped into clusters rather than evenly spread throughout the band of degeneration. Short dashed lines indicate fiber degeneration; dots indicate preterminal degeneration. Fink-Heimer procedure.

tances within VPL (Fig. 14) and, for most of their length, they follow the gentle curve of the EML. Small-diameter fibers were shorter and less regular in their course through VPL than the thick fiber, and the thin fibers had no predominant orientation. Some large fibers bend medially or laterally when they come in contact with the thick thalamocortical bundles. Some of those fibers which bend resume their rostrocaudal course by turning again and passing through the thalamocortical bundle.

We took especial note of the collateral branches and the presence of terminal clusters on the ascending axons in VPL (Figs. 14, 15). Many of the axons—particularly the large-diameter axons (although it may be because they are the easiest to see)—have collateral branches (Fig. 15B). The collaterals leave the parent axon at a wide variety of angles. The most acute angles are seen in those axons which branch from the parent axon and appear to run caudally in VPL (Fig. 14). Some large-

diameter axons appear to weave through the section, bending first medially, then laterally. Many of the collaterals run parallel to the parent axon but angle across many laminae before passing out of the section. A few axons were observed to run medial to lateral within VPL, giving off rostrocaudal branches as they went. Occasionally the parent axon itself will bend either medially or laterally and continue running parallel to EML but in a different lamina. It is not certain what proportion of the ascending afferents collateralized in such fashion because we do not know what proportion of the afferents have been filled by HRP. From existing data the typical pattern seems to be one of long axons that follow the laminar pattern for long lengths of their course through VPL but at some point deviate from a strict compliance to the rows of cell bodies. Most collaterals could not be followed very far.

Structures that appear to be terminal clusters also were observed in the antegrade HRP

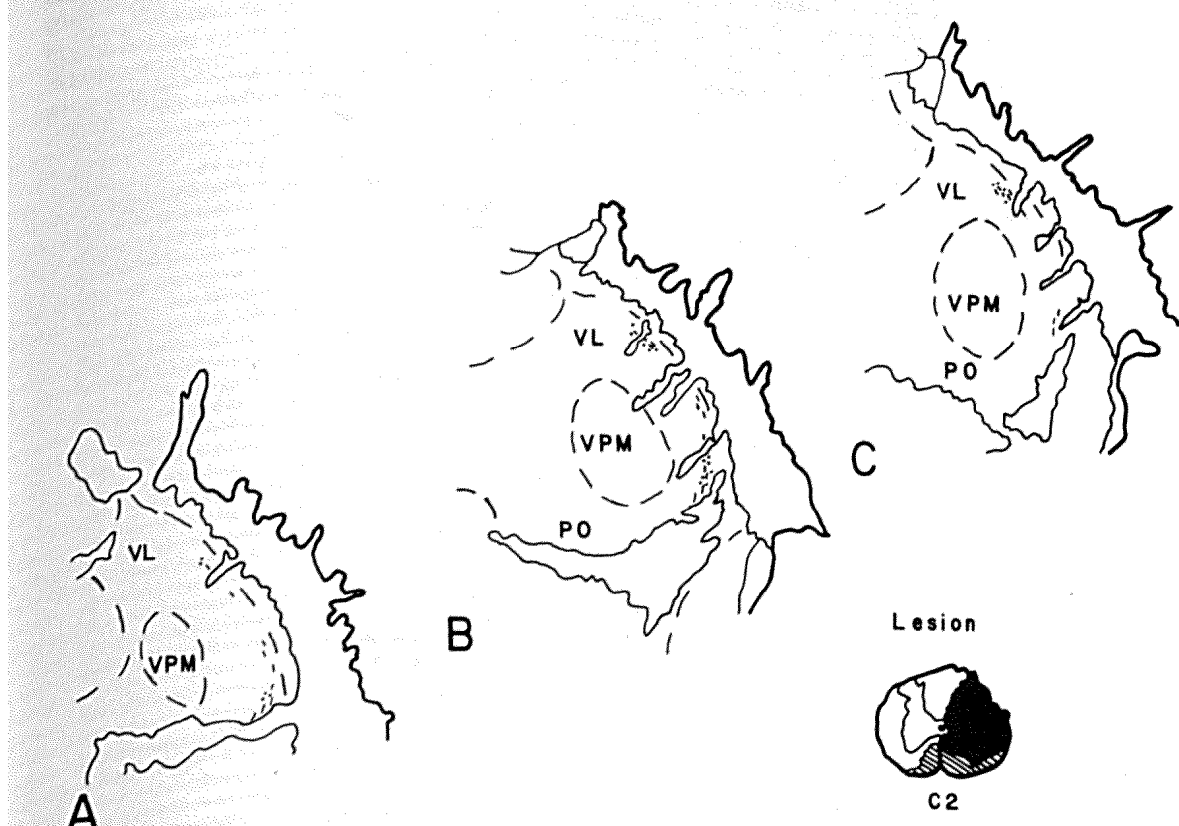


Fig. 10. Drawing of horizontal sections through three dorsoventral levels of the thalamus showing the distribution of the degeneration in VPL following the spinal cord lesion shown in the inset on the lower right. The lesion was almost a total hemisection of the cord at C2-C3. The black area indicates the area totally destroyed and the shaded area indicates the region partially destroyed. Some dorsal column

fibers appeared to be spared near the midline. The pre-terminal degeneration is found only in the rostral and caudal transition zones. The only degeneration noted in VPL was a few fibers along the lateral margin of VPL. Short dashed lines indicate fiber degeneration. Dots indicate preterminal degeneration. Fink-Heimer procedure.

experiments (Figs. 14, 15). We have not yet confirmed these structures to be terminals by other techniques so their identification remains tentative, but using criteria from the light microscope they appear to be the size and distribution of the clusters seen after Fink-Heimer stains and some appear to have bulbous endings much like those observed using Golgi stains of lemniscal afferents (Scheibel and Scheibel, '66a,b; Ramón y Cajal, '66). The clusters can be observed best in areas that are not dense with labeled axons and they frequently contain branches of various diameters which may indicate multiple inputs into a cluster. In horizontal sections the clusters were roughly circular with a width of about 35–60 μm , and, in a single section, seemed to be associated with about three to five neurons. In these preparations clusters were usually separated from each other by a gap that was at least the width or a

multiple of the width of a single cluster. Thus, from the center of one cluster to the center of the next cluster medially was either about 75 μm or about 150 μm .

Because of the collateralization of the axons and the distribution of terminal clusters, we conclude that the afferent fibers only superficially conform to the VPL lamination. The terminal arborizations and collateralization of individual fibers diverge across many rows of VPL neurons and are in fact not laminated. This conclusion is also supported by the widespread distribution of degeneration seen after punctate DCN lesions.

Synaptology

We have attempted to define the structural synaptology of VPL as it relates to the dendritic morphology, cytoarchitecture, and the sug-

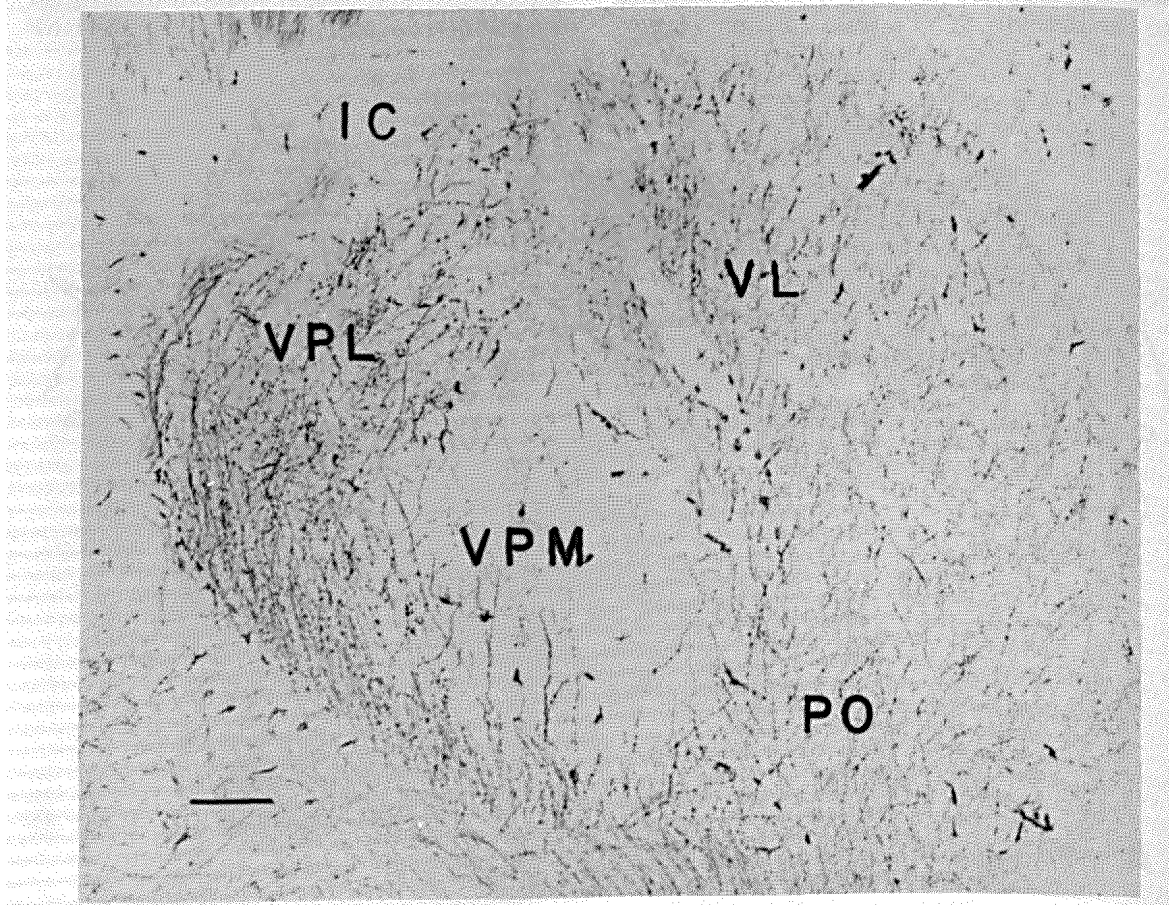


Fig. 11. Photomicrograph of a horizontal section through the lateral thalamus showing the distribution of axons containing HRP following a mesencephalic injection. In this section two pathways can be seen. The lateral pathway consists predominantly of large-diameter fibers which pass lateral to VPM and curve rostrally into VPL. The medial path-

way consists of smaller-diameter fibers and spreads out into PO, the medial nuclei, and VL. In other animals VPM contained many large-diameter fibers. A major component of the medial pathway appears to be the dentato-rubro-thalamic tract and a major component of the lateral pathway appears to be the medial lemniscus.

gested lamination of the nucleus. Our samples for electron microscopy were taken from the lateral part of the middle of VPL and thus do not contribute to our data on the transition zones but are from the areas that appear to be most laminated. All of the synapses in VPL can be categorized as one of only three types (Fig. 16); a small terminal with round vesicles and an asymmetric membrane density (SR terminal); a large terminal with round vesicles and asymmetric membrane density (LR terminal); and a terminal with many flattened vesicles (F terminal). The quantification of the synapses relates only to the neuropil as defined in Methods, i.e., without cell bodies, myelinated axons, blood vessels, and glial processes.

All of the terminals together occupy 20.6% of the area of the neuropil and occur at a frequency of 30.7 ± 2.2 terminals/ $100 \mu\text{m}^2$.

SR terminal. The terminals with round synaptic vesicles have a single asymmetric membrane density and are unencapsulated by glia. The small terminals are most frequently encountered ($24.7 \pm 1.1/100 \mu\text{m}^2$), comprising 80.5% of all synaptic profiles. The SR terminals also occupy 8.6% of the neuropil area, which is

slightly more than any of the other terminal types. The small terminal synapses on small dendrites. Histograms of the average diameter of dendrites on which they synapse (Fig. 17) show that both terminals and dendrites are from a population with a mean diameter of $0.65 \pm 0.02 \mu\text{m}$. The small dendrites correspond to the distal dendrites of the typical VPL neuron.

Lesions placed in the neocortex, medial lemniscus, dorsal column nuclei, and the spinal cord indicate that some of the SR terminals come from cells of the cortex (Fig. 18). When lesions are placed in somatosensory cortex, SR terminals degenerate. With large cortical lesions 21% of the SR terminals are lost. The sources of the remaining 79% of the SR terminals are unknown for this middle region of VPL.

LR terminals. Very large terminals averaging $2.19 \pm 0.06 \mu\text{m}$ in diameter are present and contain round synaptic vesicles (Fig. 16). Some of these terminals are as large as 5–6 μm in diameter. Although conspicuous in size, these terminals comprise only 4.9% of all terminal types and occur with the lowest frequency of 1.5

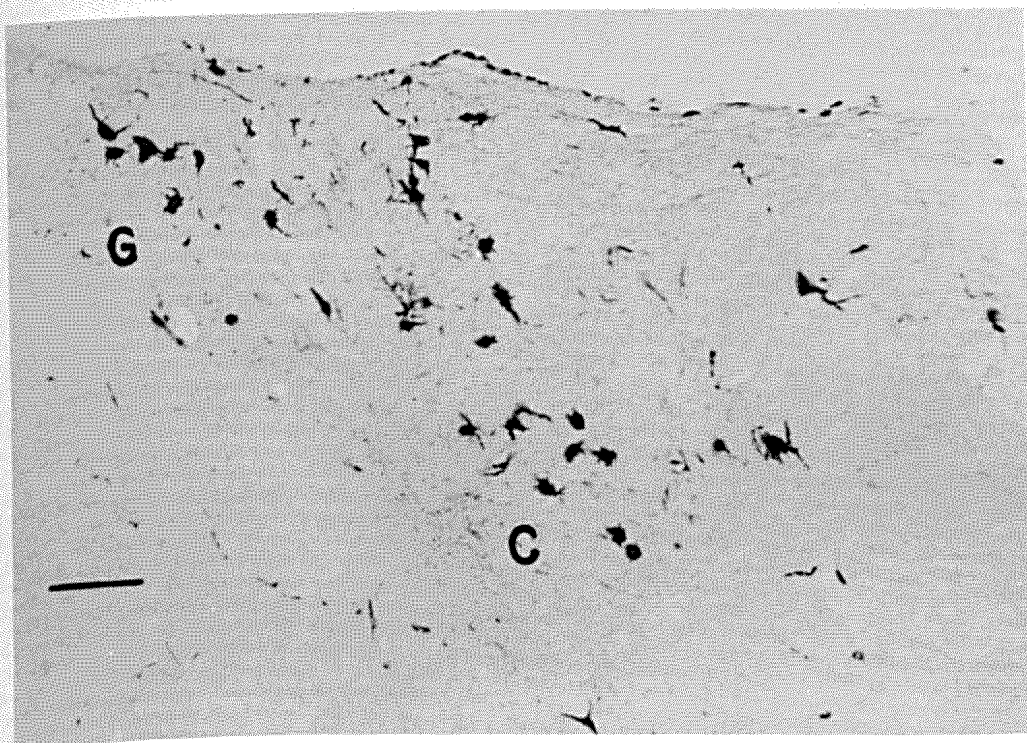


Fig. 12. Photomicrograph showing the retrograde transport of HRP, the nucleus gracilis (G), and nucleus cuneatus (C). The injection site was in the ventral mesencephalon and retrograde transport occurred in many other nuclei including the trigeminal nuclei, spinal cord, reticular formation, and deep cerebellar nuclei. Coronal section. No counterstain. Bar, 50 μm .

terminals/100 μm^2 . LR terminals are ensheathed by a glial capsule. There are two kinds of membrane thickening in the LR terminal of which only one is associated with synaptic vesicles. The membrane density associated with vesicles occurs most frequently on the dendritic appendages and is asymmetric. The other type of dense membrane occurs along the major shaft of the dendrite and appears to be puncta adherentia. Although the LR terminal occurs least frequently, it occupies 5.8% of the area of neuropil, which is only slightly less than that occupied by the SR terminal.

The LR terminal synapses on a dendrite that has an average diameter of $2.10 \pm 0.08 \mu\text{m}$. As shown in the histogram (Fig. 17), the LR terminal has a wide range of diameters but there is only the slightest overlap with the population of dendrites on which SR terminals were found. This probably reflects the abrupt change in diameter from proximal to distal dendrite that occurs at the whorl. The LR terminal, there-

fore, synapses on the proximal dendrites and not on distal dendrites. A few LR terminals have been observed at sites where it is difficult to distinguish cell body from proximal dendrite but were not included in our quantification.

Two to 6 days after ablations of the contralateral DCN (Fig. 19) an average of 46.7% (range: 37.5–75%) of all LR terminals are lost. Two and 3 days after such lesions, the round vesicles and multiple synaptic junctions of the large terminals can still be identified (Fig. 19). Approximately 6 days after the DCN lesions, unoccupied postsynaptic densities can be seen on large-caliber dendrites, and the vacant sites are covered by a glial process. There was no apparent correlation between the size of the DCN lesion (determined by planimetry from serial sections) and the number of LR terminals surviving, although there was a rough correlation with the amount of gliosis produced in VPL. Large lesions of the ipsilateral medial lemniscus at the pontomedullary junction

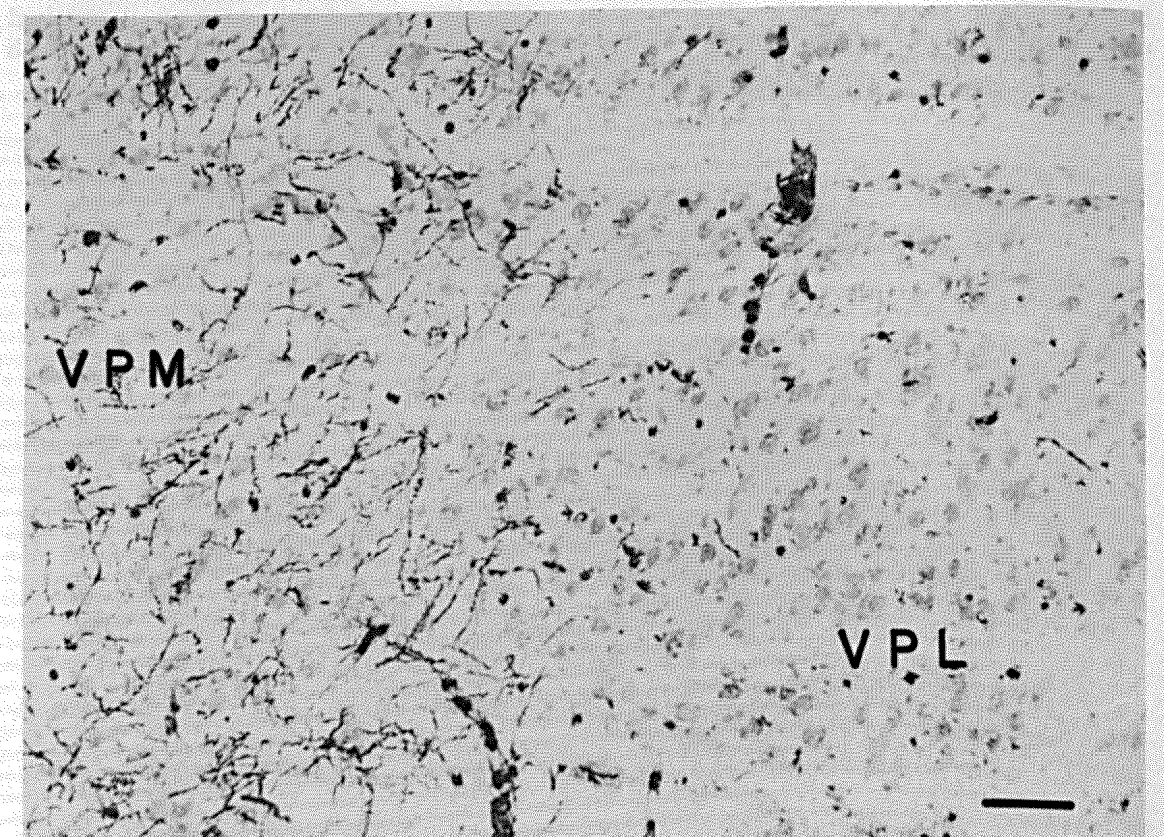


Fig. 13. Photomicrograph of a horizontal section through VPM and VPL. A large lesion of the DCN was made prior to the mesencephalic injection of HRP. No fibers in VPL contain HRP but many fibers in VPM show the label. Mesulam's TMB method with neutral red counterstain. Bar, 25 μm .

cause a greater degree of degeneration of the LR terminals with an average of 80% among all animals, although one animal lost as many as 92% of all LR terminals.

F terminals. The third type of synaptic terminal (F) found in VPL contains many flat vesicles that are slightly smaller than the round vesicles (Fig. 16). F terminals are of intermediate size (1.23 μm in average diameter), and make single contacts with symmetrical mem-

brane densities on postsynaptic dendrites that average 1.57 μm in diameter. Because F terminals may contact dendrites of a wide variety of diameters ranging in size from 0.5 to about 3 μm in diameter (Fig. 17), it appears that F terminals form synapses on both proximal and distal dendrites. The F terminal is rarely encapsulated by glial processes, and the vesicles are closely packed together in a rather electron-dense cytoplasm. A few F terminals are



Fig. 14. Photomicrograph of axons in VPL following the anterograde transport of HRP from a mesencephalic injection. Lateral is to the left of the photograph. Large-diameter axons course through VPL giving off collaterals (c). In this instance the collaterals are angled caudally. Small-diameter fibers

can also be seen containing HRP. Some axons seem to contribute to configurations which appear to be terminal arborizations (ta) or clusters. Closed arrow points rostrally and is aligned with the VPL laminae. Bar, 25 μm . No counterstain.

observed which have synaptic contact with more than one dendritic profile. The F terminals are 14.6% of the total number of synapses, occupy 6.3% of the area of neuropil, and are observed with a frequency of $4.5 \pm 1.05/100 \mu\text{m}^2$.

Attempts have been made to identify the source of the F terminals but the results are inconclusive. No degenerating F terminals have been observed after any cortical, DCN, or spinal cord lesion.

Synaptic arrangement. Some F terminals have an obvious close association with the LR terminal on the proximal dendrite. The F terminal is always adjacent to the LR terminal but did not penetrate the glial capsule of the larger terminal. No SR terminals are seen on the proximal dendrites. Complex synaptic arrangements commonly seen in other nuclei in the rat and in the VPL of other animals are not observed in the VPL of the rat. There are no axoaxonic synapses, dendrodendritic synapses, or triadic or other serial synaptic arrangements. A few synapses of the F and SR type occur on the cell body of several VPL neu-

rons, and single F and SR terminals had infrequent multiple synaptic contacts with different synaptic profiles.

DISCUSSION

Cytoarchitecture

The cytoarchitectonic borders of the ventrobasal complex have been defined in the rat by a number of authors, notably Lund and Webster ('67a,b), Jones and Leavitt ('74), and Faull and Carmen ('78). Within the main body of the ventrobasal complex, a lateral subdivision can be recognized that corresponds structurally (Lund and Webster, '67a) and functionally (Angel and Clark, '75) to VPL. Difficulties arise, however, when one attempts to define either the rostral or caudal boundaries of VPL. It is now recognized that the posterior thalamic complex (PO) forms the caudalmost boundary of the thalamic ventral tier nuclei (Jones and Leavitt, '74). The transition, however, between caudal VPL and lateral PO (POI) is cytoarchitecturally vague. There is no appreciable difference in cell densities, and the change from the larger, discoid multipolar cells in VPL to the smaller, more

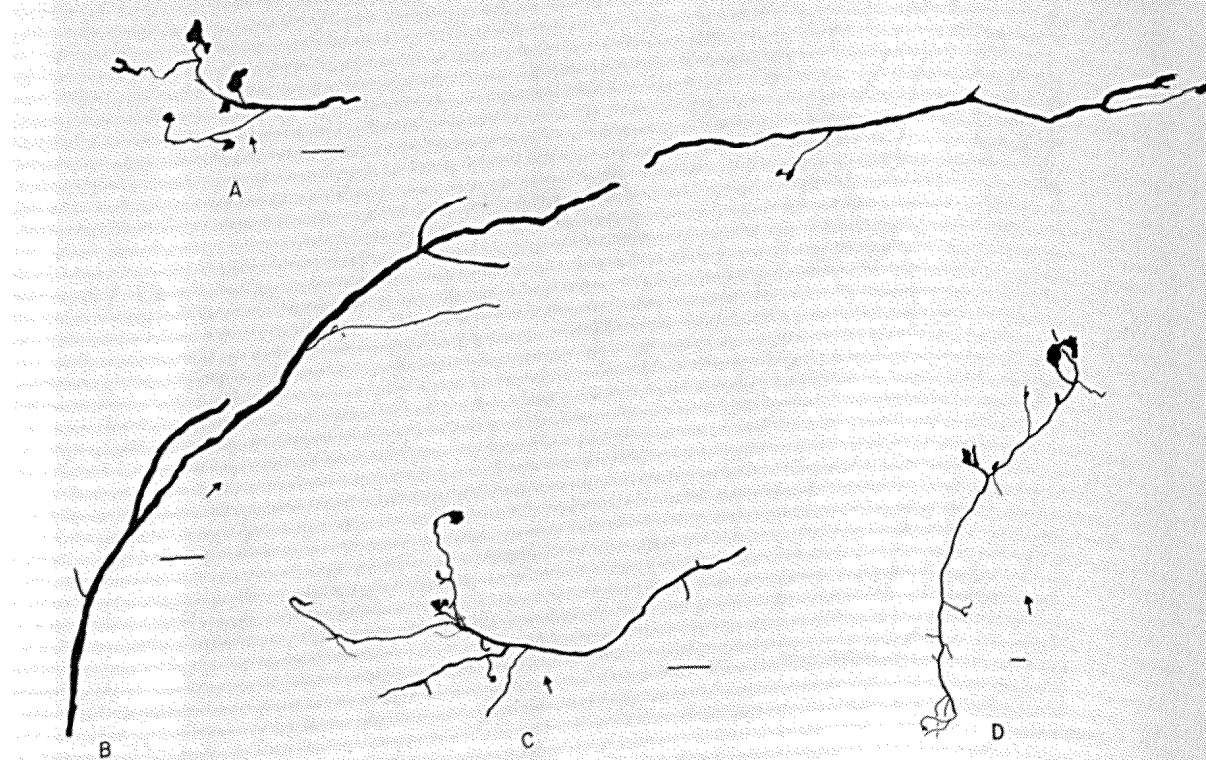


Fig. 15. Drawings of HRP-filled axons from VPL showing three terminal arborizations in A, C, and D and a parent axon that courses for a long distance through VPL in B. Most of the collaterals of the parent axon begin to course rostrally.

Closed arrow is pointing rostrally in each of these horizontal sections but in A, C, and D lateral is to the right of the figure while in B it is to the left of the figure. No counterstain. Bar, 25 μm .

rounded multipolar neurons that populate PO is so gradual that it is barely noticed. Our preliminary Golgi analysis of PO indicates that the neurons of POI exhibit a dendritic morphology intermediate to that of typical VPL neurons and the cells more frequently observed in more medial parts of PO (McAllister et al., '78). Thus, POI neurons usually have longer, more extensively branched dendrites than their medial counterparts, yet they seldom exhibit the whorl branching pattern that typically produces dendritic sheaves in VPL. Clearly, this region requires more detailed study before its morphological character and limits can be described with certainty.

Our suggestion that the caudal pole of VPL blends cytoarchitecturally with POI does have some interesting connectional and neurophysiological correlates. The focus of degenera-

tion in the caudal transition zone reported here confirms the earlier reports of Lund and Webster ('67a,b), that both DCN and spinal projections converge upon the caudolateral portion of VPL. Since our spinal hemisections were restricted to high cervical levels, it is impossible to segregate spinothalamic and spino-cervicothalamic components of this terminal field. Lund and Webster ('67b) did not report such a terminal field with any lesion below the C3 level, and thus considered the possibility that the neurons projecting to this area were confined to the lateral cervical nucleus (LCN) located at C1 and C2. Giesler et al. ('79) have investigated the origin of LCN in the rat by injecting HRP into the VB complex and have supported the previous results that LCN is located in the rostral levels of spinal cord. The overlap of lemniscal and spinal projections in



Fig. 16. An electron micrograph of the neuropil of VPL. The three types of terminals can be seen here. There is a large, round-vesicle terminal (LR) which synapses on a large-diameter dendrite. The synapse usually occurs on a dendritic appendage (closed arrowheads). Nonsynaptic contacts between the two profiles also occur (open arrowheads) and appear similar to puncta adherentia. A second type of

terminal synapses on the large-diameter dendrite. This terminal has many flattened vesicles and a symmetric membrane density at the contact site (F). A small, round-vesicle terminal is also found in the neuropil and synapses on small-diameter dendritic profiles (SR). The latter terminals have an asymmetric membrane density at the synaptic contact. Bar, 1 μ m.

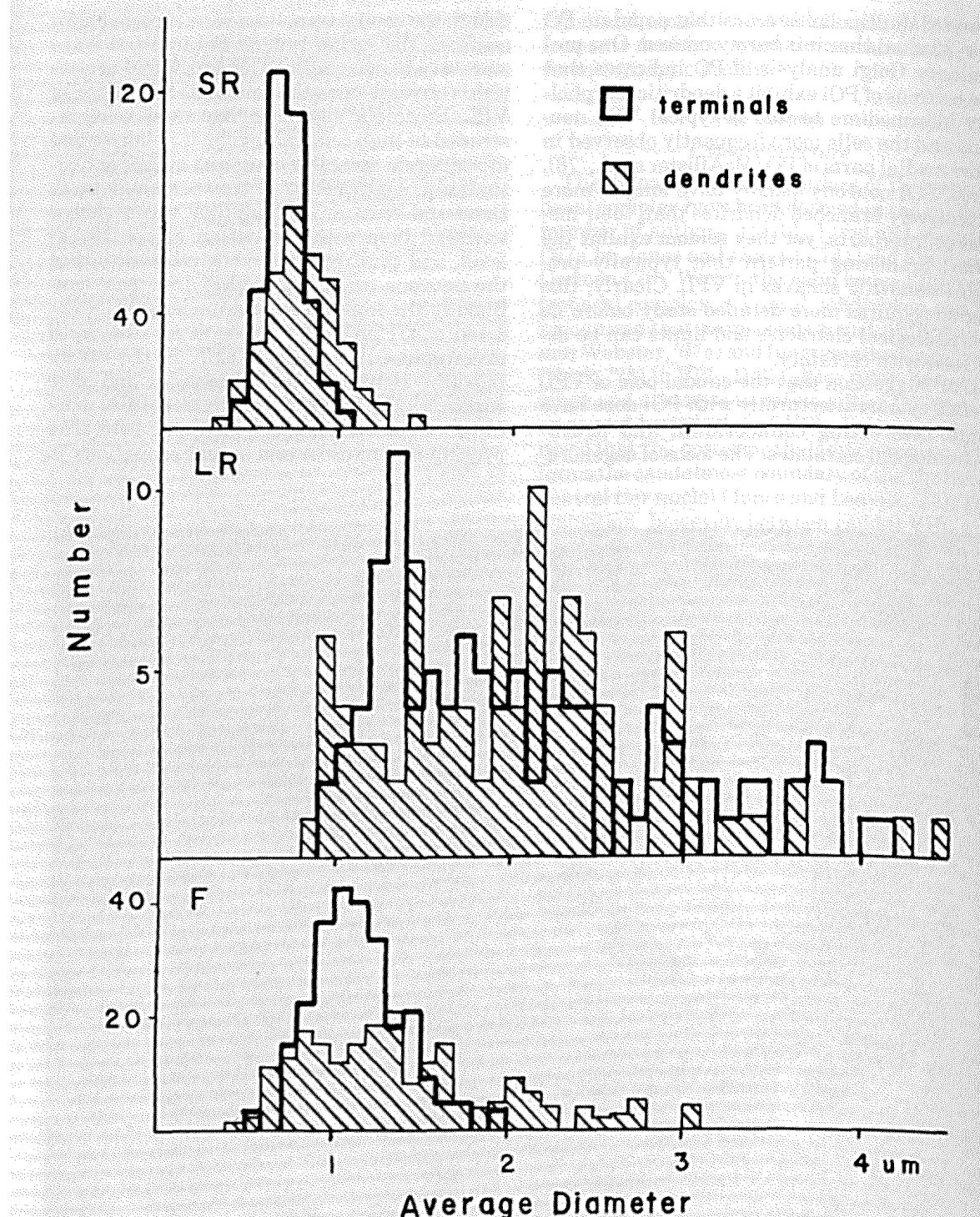


Fig. 17. Histogram showing the average diameters of the three terminal types in the VPL neuropil and the dendrites on which they synapse. This histogram demonstrates that the small terminals (SR) synapse on small dendrites, the large terminals (LR) synapse on large dendrites, and the terminals with many flattened vesicles (F) synapse on both large- and small-diameter dendrites. Very few SR terminals synapse on dendrites greater than 1 μm .

and very few LR terminals synapse on dendrites less than 1 μm . The separation is probably greater because the average diameter (average of greatest and least diameter) tends to overestimate the actual diameter of the dendrites. The abrupt change in diameter between proximal and distal dendrites is also reflected in the relative paucity of overlap in the SR and LR histograms.

caudal VPL correlates well with the evoked response studies that indicate a probable zone of convergence within this same region (Davidson, '65; Angel and Clark, '75). There is a general agreement among these authors that caudolateral portions of the ventrobasal complex contain a preponderance of neurons that exhibit large cutaneous receptive fields and respond to either bilateral or multiple limb stimulation. Consequently, Emmers ('65) has referred to this region as the SII component of the rat thalamus. In contrast to those who consider the neurons with large, often bilateral receptive fields to be contained within the VB complex, Davidson ('65) includes this region within the posterior thalamic complex, in "an area caudal to and partially co-extensive with the ventrobasal complex." Thus, our cytoarchitectural observations lend morphological support to the view that the SII region or the "zone of convergence" within VB is confined to a transitional area that includes caudal VPL and POI.

The possibility that VPL and POI neurons coinhabit the caudal pole of VPL gains further support from the horseradish peroxidase experiments of Saporta and Kruger ('77). Following discrete injections of HRP into physiologically identified regions of SI cortex, they found retrogradely labeled neurons in caudal and ventral portions of VB that intermingled with unlabeled neurons. This pattern contrasted sharply to that seen at more rostral levels in which "all neurons, covering the variety of shapes and sizes of VB neurons, were labeled." Furthermore, the density of labeled HRP neurons in caudal VB could not be increased with cortical injections of larger size. Thus it is conceivable that these unlabeled neurons represent POI cells that interdigitate with the thalamocortical relay cells of VPL.

Determination of a cytoarchitectural boundary for the rostral pole of VPL is just as elusive as that of the caudal limit. Once again, the results of our degeneration experiments appear

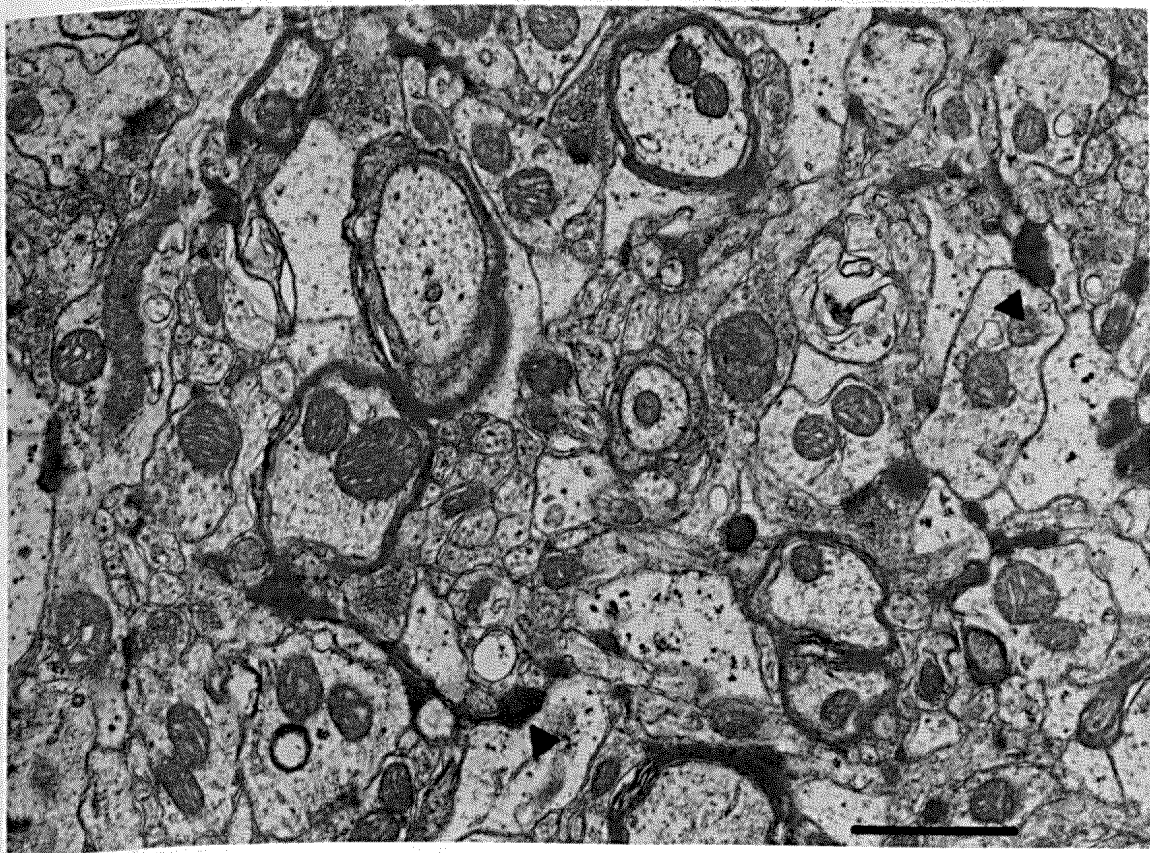


Fig. 18. Electron micrograph of the neuropil in VPL four days after a lesion of the somatosensory cortex. Dense degeneration of small terminal profiles (closed arrowheads) can be seen throughout the neuropil. About 20% of the SR terminals are lost following cortical lesions. Bar, 1 μ m.

to be in close agreement with those of Lund and Webster ('67a,b). Unfortunately, we can only infer that our terminal degeneration coincides with the location of similar projection patterns found by Lund and Webster ('67a,b), since they do not correlate their schematic drawings with cytoarchitectural details and rely on an unpublished atlas for nuclear delineations. This becomes a significant problem when we attempt to define the rostral boundary of VPL on the basis of both cytoarchitecture and connectivity. Our results indicate that both the DCN and spinal projections extend rostrally beyond VPL into adjacent regions of VL. This overlap is most apparent in horizontal sections. Rostral to VPL, the VL nucleus, as defined by its afferent projections from the cerebellum (Chan-Palay, '77; Faull and Carmen, '78; Faull, personal communication), expands to fill the remainder of the ventral tier nuclear group. In these horizontal sections it can be clearly seen that the

DCN projection curves medially and continues rostrally into the caudolateral part of VL. The degeneration from spinal lesions remains compressed against the external medullary lamina, until it reaches the rostral transition zone where it expands rostrally into lateral portions of VL. Antegrade HRP experiments are particularly useful in determining nuclear boundaries, since the cytoarchitectural and fiber pattern can be viewed simultaneously in counterstained material. Such preparations that had received injection into the ventral mesencephalon verify the overlap into VL. In the cat, the transition zone between VL and VPL projected exclusively to somatosensory cortex (area 3a) and therefore was thought to be part of VB rather than VL (Strick, '73).

The rostral limits of both the DCN and the spinal terminal fields are particularly difficult to interpret in transverse sections, because the neurons of VPL appear to intermingle with

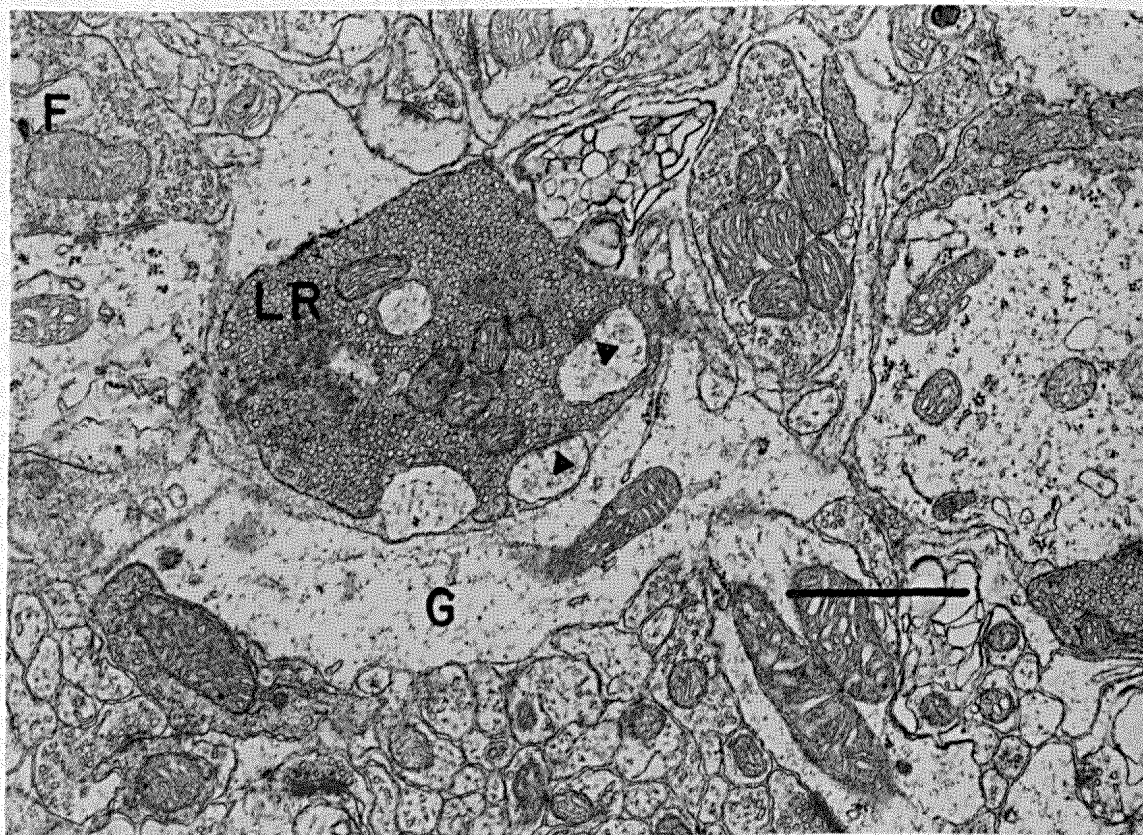


Fig. 19. Electron micrograph from the neuropil of VPL 1 day after a lesion to the DCN. The LR terminal is beginning to undergo dense degeneration. Synaptic densities on the dendritic appendages can still be observed (closed arrowheads). A nearby F terminal remains intact (F). During the

process of degeneration the glial processes (G) swell. The number of LR terminals is reduced by DCN lesions but no sign of degeneration is seen in any other terminal type. Bar, 1 μ m.

those of VL. Nevertheless, we support the nuclear delineations advanced by Faull and Carmen ('78), and illustrated by Jones and Leavitt ('74). VPL does not occupy the rostrocaudal extent of the ventral tier. Within an area 200–500 μm caudal to the rostral pole of VL, terminal degeneration is seen after DCN and spinal lesions. The DCN and spinothalamic projections reported by Lund and Webster ('67a,b) seem to include this same area, but this comparison is uncertain because their delineations of VL differ from ours and their schematic drawings do not show the entire rostral pole of their ventral tier nuclei. Within this area, most neurons are either round or oblong in shape, in contrast to the markedly elongate somata observed in intermediate portions of VPL.

Dendritic morphology

The dendritic morphology of thalamocortical relay neurons (TCR) has been previously described in generalized fashion for several mammalian species, principally mouse, rat, and cat (Ramón y Cajal, '11, '66; Scheibel and Scheibel, '66a; Tömböl, '66/67; Scheibel et al., '72ab, '73, '76). It has been reported that these neurons elaborate four to ten principal dendrites, each of which branches repeatedly within a short distance to form a sheaf of secondary or tertiary dendrites. All reports to date have either illustrated or described these TCR neurons as having spherical dendritic fields formed from primary dendrites that radiate in all directions from the soma. Collectively, the sheaves of distal dendrites impart a "bushy" character to the dendritic field, prompting Ramón y Cajal ('11) to refer to this type of neuron as a "Buschzell." These neurons can be found in varying degrees, depending primarily on species, in all specific relay nuclei of the thalamus. Since axons of these large neurons enter fiber bundles that appear to leave the various nuclei, they most certainly are the projection neurons of the thalamocortical relay system. The comprehensive reports of the Scheibels' (Scheibel and Scheibel, '66a; Scheibel et al., '72c) are based on the VB complex as a whole, with no mention of regional differences between VPM and VPL. Furthermore, these studies focus primarily on either the pattern of afferent input to the ventrobasal complex (Scheibel and Scheibel, '66a,b; Scheibel et al., '72c; Scheibel et al., '73), or upon the intrinsic organization of the complex itself (Scheibel et al., '72a,b), and admittedly only present broad descriptions of the individual cell types.

The developmental study of Scheibel et al. ('76) does describe the maturation of TCR cell dendritic fields, but does not specifically examine VPL or VPM separately, nor does it seem to include any rat thalamic tissue older than 28 days of age. While certain axonal features can only be visualized if the Golgi method is applied to neonatal rats, prior to myelination, it remains possible that some further dendritic differentiation may occur up to adulthood. However, Tömböl employs the perfusion Golgi-Kopsch method (Szentágothai, '63) to specifically impregnate adult tissue. Although her conclusions are based on the observations of several different thalamic relay nuclei, she is careful to itemize individual variations when they occur and has limited her Golgi analysis to the cat. Most of the other investigations rely on a compilation of observations made on rodent and feline material in an effort to summarize VB dendritic and axonal morphology.

Our observations indicate that while the neurons that populate VPL do share some common dendritic features with the generalized pattern ascribed to all TCR neurons, significant differences do occur. The branching patterns and orientation of dendrites that characterize TCR neurons seems to be faithfully represented only in those cells that comprise VPM. Their large spherical dendritic fields and sheaves of distal dendrites are nearly identical to the structural features repeatedly illustrated by the Scheibels (see Fig. 1A of Scheibel et al., '72c). In contrast, VPL neurons exhibit three conspicuous modifications of the generalized pattern. First, the somata of VPL neurons are somewhat smaller than those found in VPM, and, more importantly they are typically discoid in shape. In horizontal sections, the long axis of these cells is oriented along a rostrocaudal plane, while in coronal sections it runs from dorsolateral to ventromedial. Secondly, the thick proximal dendrites of VPL neurons frequently generate distal dendrites in a whorl pattern of branching. This distinctive feature results when a proximal dendrite ends abruptly and gives rise to distal (secondary or tertiary) dendrites with markedly reduced diameters. At first glance the TCR cells described by others, as well as the VPM neurons encountered in our material, appear to branch in the same manner to produce tufts of distal dendrites. Closer examination, however, reveals that these neurons produce their tufts by generating distal dendrites through a rapid sequence of closely spaced alternate branch points, and not in a whorl pat-

tern at all. Occasionally VPL neurons may exhibit an alternate branching pattern, but the whorl pattern so frequently seen in VPL has not been observed in VPM. Thirdly, the orientation of both proximal and distal dendrites results in dendritic fields within VPL that are predominantly fusiform, or flattened in shape, and these dendritic fields are conspicuously aligned parallel to the EML. This contrasts sharply with the radial proximal dendrites and spherical dendritic fields that the Scheibels (Scheibel and Scheibel, '66a; Scheibel et al., '72c) and Tömböl ('66/67) describe, and which we too have noted in rat VPM. More recently (Scheibel et al., '72c), and in an earlier study of the ventral anterior thalamic nucleus (Scheibel and Scheibel, '66b), the Scheibels noted the presence of multipolar neurons with dense flattened dendritic domains that emanated from opposite poles of the soma. This cell type was found along the lateral margins of the VA nucleus, and hence was termed a "marginal" neuron. These same authors found neurons with morphological features that were nearly identical to those of "marginal" cells, located infrequently within the VB complex of the cat, but which due to their restricted axonal domains were considered local circuit neurons. It is possible that those "marginal" neurons are displaced VPL neurons as in the transitional zone of the rat.

On the basis of dendritic morphology, no Golgi type II neurons were detected in the rat VPL. Local circuit neurons have been defined by the pattern and extent of their axonal plexuses in previous studies, primarily in the cat (Scheibel and Scheibel, '66a; Scheibel et al., '72a,b,c; Tömböl, '66/67, '69b). In these reports, nearly all Golgi type II neurons were shown to possess sparsely branched dendrites with more frequent and elaborate appendages. Only in caudal parts of rat VPL, where the nucleus appears to blend with POI, could neurons be found with short, relatively unbranched dendrites and radiate dendritic fields.

Synaptology

The synaptic neuropil in the rat VPL is unusual in its relative simplicity. It has none of the complex synaptic arrangements seen in the cat VPL (Ralston and Herman, '69; Ralston, '71) or even other relay nuclei in the rat (e.g., the lateral geniculate, Lieberman, '73). Previous studies have shown that there are only three types of terminals in the rat VPL (Špaček and Lieberman, '74; Matthews and Faciane, '77; Tripp and Wells, '78). Of the total number

of terminals, the SR terminal comprises 80%, the F terminal 15%, and the LR terminal, which is thought to represent the major somatosensory input to VPL, only 5% of the total. Based on our data of the average diameters of the dendritic profiles receiving these terminals, we have concluded that the SR terminal synapses on distal dendrites, F terminals on both proximal and distal dendrites, and the LR only on proximal dendrites. LR terminals occasionally synapsed on the cell soma or at the base of the proximal dendrite, where it is difficult to determine the difference between soma and dendrite. Some SR and F terminals were also seen on the soma but our sampling procedures did not allow us to quantify them.

Are there intrinsic neurons in the rat VPL?

Evidence from several studies, using a variety of techniques, when viewed collectively, supports the conclusion that interneurons are absent from the rat VPL. Both Ramón y Cajal ('66) and Scheibel and Scheibel ('66a), using Golgi staining methods, noted that there were no neurons in the rat and mouse whose axons stayed completely within the ventrobasal complex. Both studies did observe intrinsic neurons in the ventrobasal complex in other species, notably the cat. In more recent years interneurons have been associated in EM with vesicle-containing dendrites in many but not all nuclei (e.g., in cat VPL, Ralston, '71). No vesicle-containing dendrites have been observed in the VPL in the rat in the present study nor in previous studies (Matthews and Faciane, '77; Tripp and Wells, '78) although Špaček and Lieberman suggest their existence but "not in significant numbers." The latter authors also suggest that vesicle-containing dendrites would be found in studies more careful than theirs, but the more recent studies have not reported such profiles (Matthews and Faciane, '77; Tripp and Wells, '78). Interneurons may also be associated with triadic or serial synapses that may not involve vesicle-containing dendrites (Famiglietti and Peters, '72), but in those EM studies in the rat or mouse cited above, serial synapses have not been observed in the neuropil. In a comprehensive study of the physiological characteristics of VPL neurons in the rat, Angel and Clarke ('75) could find no neurons from a sample of 998 neurons that showed the physiological characteristics of interneurons described by others in other locations. Using yet another technique, Saporta and Kruger ('77) found that when they placed HRP into a small area of the somatosen-

sory cortex, a coherent band of neurons was retrogradely labeled in the rat VB except in the rostral and caudal transition zones. They noted that all of the neurons within that band in VPL were labeled, implying that all of the VPL neurons projected to cortex and that there were no interneurons in VPL. These studies, while not sufficient individually, when taken together suggest that it is perhaps more appropriate to develop a structural plan for the processing of somatosensory information in VPL in the rat that does not include an intrinsic neuron in the circuit.

Structural plan of VPL

The input from the DCN to VPL in the rat is collateralized, widespread, and the terminals are not in conformation with the curved laminae of VPL. The punctate lesions of DCN showed that clusters of degenerating terminals extended in a broad band throughout VPL and the results of the antegrade transport of HRP also showed collaterals and a lack of conformity to the layers of VPL. Studies using Golgi-stained material from young mice and rats (Scheibel and Scheibel, '66a; Ramón y Cajal, '66) have illustrated terminal arbors at the ends of collaterals but the extent of the collateralization has been difficult to determine from their published illustrations. In a study of the rat ventrobasal complex using electron microscopy, Lieberman et al. ('72) observed a myelinated axon which gave rise to at least six other myelinated branches. The clusters which we observed after the antegrade transport of HRP seemed to conform to a laminar pattern but the laminae were wider (about 35–40 μm) than the individual rows of TCR neurons (about 10 μm). Because of the collateralization of the DCN input, a single DCN fiber presumably may provide input to several clusters at widely separated places in VPL. It would appear then that collaterals of the DCN input are an important feature of the structural plan for VPL in the rat. In the cat, Hand and Van Winkle, ('77) have demonstrated that clusters of degenerating terminals from collaterals of DCN axons occur in the VPL but seem to be more localized in the cat and do conform to some general kind of laminar pattern. The latter investigators also indicate that DCN input may overlap with input from other parts of DCN or from other sources. The major difference in the distribution of the DCN input between the rat and the cat seems to be that an individual DCN neuron in the rat contributes to a wider and more extensive array of clusters than those of the cat. The cluster in the rat, in all likelihood, does not

have intrinsic neurons that can be used in selective inhibition. Within the cluster in the rat, there are likely to be multiple inputs from DCN and those inputs synapse on proximal dendrites while the inputs from cortex synapse on distal dendrites.

The lack of complexity in the rat VPL creates an unusual situation in the somatosensory system of the rat because the neuropil of the DCN is much more complicated than that of VPL. The input to the DCN of the rat is also collateralized particularly from the primary afferents (Gulley, '73). The DCN processes incoming information by a very different structural circuit than does VPL. Studies of the DCN have demonstrated the presence of intrinsic neurons (Gulley, '73) and serial synapses, some of which appear to be vesicle-containing dendrites (Tan and Lieberman, '78; Wells, unpublished observations). In the cat, a similar structural plan for the DCN has been observed by Rustioni and Ellis ('78), and these authors suggested that the serial synaptic arrangements accounted for the surround inhibition from primary afferents because nonprimary afferents had no surround inhibition and also did not participate in serial synapses.

In the most comprehensive study of the response properties of VPL neurons in the rat, Angel and Clarke ('75) have shown that somatotopy, modality separation, and small receptive fields can be generated among the neurons of VPL following stimulation of the periphery. This implies that the VPL input must be organized in a way that will permit the focusing of divergent information without the structural basis for surround inhibition or presynaptic inhibition (there are no axoaxonic synapses). Angel and Clarke ('75), recognizing the likelihood that there are no interneurons in VPL, have suggested that the collateralized inputs interact in such a way as to produce a "surround facilitation." They found that the neurons with the smallest receptive fields responded with a slightly longer latency than those with larger receptive fields (in contrast to the cat; Harris, '78), although both were localized to the contralateral foot pad. This suggested to them that the delay in latency may have allowed summation from the input of the wider fields with that of the smaller field in order to generate the excitation of the small field neuron. Their model of the structural plan of VPL depends fundamentally on a highly collateralized input of rapidly conducting fibers (presumably from DCN) to VPL and has the advantage of not requiring serial synapses for

normal functions to occur.

There are some important pieces of the structural plan of VPL that are missing. In order to complete the connectivity of the rat VPL one needs to obtain information on the pattern of distribution of the DCN collaterals of individual DCN neurons whose response properties are known. It will also be important to determine the degree of convergence on a particular VPL neuron or cluster of neurons by different DCN neurons. In addition the source(s) of the F terminal should be sought since they may be a source of feed forward inhibition that may parallel the DCN input and provide some of the inhibitory input needed to generate narrow fields and modality separation. In fact, the source of the remaining terminals which have not been characterized (25% of the LR terminals and 80% of the SR terminals) should be determined. The chances for determining a complete structural plan for VPL are enhanced because the rat VPL has a limited input, no interneurons, only three terminal types, and no complex synaptic arrangements. Once the structural plan is complete for VPL its capabilities can be compared to those of DCN, which has a more complicated plan, and problems can then be addressed which pertain not only to the processing of somatosensory information but also to other neurobiological problems of connectivity.

ACKNOWLEDGMENTS

The authors are grateful to L.N. Tripp for collaboration and technical assistance, to D.K. Ryugo for some Golgi material, to W.G. Bolldosser for technical assistance and photography, and to S. Carrington and C. Foote for preparation of the manuscript.

Portions of this study were supported by PHS 5429-17-3 and by a University of Vermont Postdoctoral Fellowship to J.P.M.

J.W. is a Sandoz Foundation Fellow in Neuroscience.

LITERATURE CITED

- Angel, A., and K.A. Clarke (1975) An analysis of the representation of the forelimb in the ventrobasal complex of the albino rat. *J. Physiol. (Lond.)* **249**:399-424.
- Bodian, D. (1936) A new method for staining nerve fibers and nerve endings in mounted paraffin sections. *Anat. Rec.* **65**:89-97.
- Chan-Palay, V. (1977) *Cerebellar Dentate Nucleus: Organization, Cytology and Transmitters*. Berlin: Springer-Verlag.
- Davidson, N. (1965) The projection of afferent pathways in the thalamus of the rat. *J. Comp. Neurol.* **124**:377-390.
- Donoghue, J.P., and J. Wells (1977) Synaptic rearrangement in the ventrobasal complex of the mouse following partial cortical deafferentation. *Brain Res.* **125**:351-355.
- Emmers, R. (1965) Organization of the first and second somesthetic regions (SI and SII) in the rat thalamus. *J. Comp. Neurol.* **124**:215-228.
- Famiglietti, E.V., and A. Peters (1972) The synaptic glomerulus and the intrinsic neuron in the dorsal lateral geniculate nucleus of the cat. *J. Comp. Neurol.* **144**:285-334.
- Faulk, R.L.M., and J.B. Carmen (1978) The cerebellofugal projections in the brachium conjunctivum of the rat. I. The contralateral ascending pathway. *J. Comp. Neurol.* **178**:495-518.
- Fink, R.P., and L. Heimer (1967) Two methods for selective silver impregnation of degenerating axons and their synaptic endings in the central nervous system. *Brain Res.* **4**:369-374.
- Giesler, G.J., D. Menétry, and A.I. Basbaum (1979) Differential origins of spinothalamic tract projections to medial and lateral thalamus in the rat. *J. Comp. Neurol.* **184**:107-126.
- Gulley, R.L. (1973) Golgi studies of the nucleus gracilis in the rat. *Anat. Rec.* **177**:325-342.
- Hand, P.J., and T. Van Winkle (1977) The efferent connections of the feline nucleus cuneatus. *J. Comp. Neurol.* **171**:83-110.
- Harris, F.A. (1978) Regional variations of somatosensory input convergence in nucleus VPL of cat thalamus. *Exp. Neurol.* **58**:171-189.
- Jones, E.G., and H. Burton (1974) Cytoarchitecture and somatic sensory connectivity of thalamic nuclei other than the ventrobasal complex in the cat. *J. Comp. Neurol.* **154**:395-432.
- Jones, E.G., and R.Y. Leavitt (1974) Retrograde axonal transport and the demonstration of non-specific projections to the cerebral cortex and striatum from thalamic intralaminar nuclei in the rat, cat and monkey. *J. Comp. Neurol.* **154**:349-378.
- Lieberman, A.R., K.E. Webster, and J. Špaček (1972) Multiple myelinated branches from nodes of Ranvier in the central nervous system. *Brain Res.* **44**:652-655.
- Lieberman, A.R. (1973) Neurons with presynaptic perikarya and presynaptic dendrites in the rat lateral geniculate nucleus. *Brain Res.* **59**:35-59.
- Lund, R.D., and K.E. Webster (1967a) Thalamic afferents from the dorsal column nuclei. An experimental anatomical study in the rat. *J. Comp. Neurol.* **130**:301-312.
- Lund, R.D., and K.E. Webster (1967b) Thalamic afferents from the spinal cord and trigeminal nuclei. An experimental anatomical study in the rat. *J. Comp. Neurol.* **130**:313-328.
- Matthews, M.A., and C.L. Faciane (1977) Electron microscopy of the development of synaptic patterns in the ventrobasal complex of the rat. *Brain Res.* **135**:197-215.
- McAllister, J.P., D.M. Fekete, J. Wells, and D.K. Ryugo (1978) The relationship of cytoarchitecture and dendritic morphology to afferent input within the thalamic ventral tier nuclei of the rat. *Soc. Neurosci. Abst.* **3**:487.
- Mesulam, M.M. (1978) Tetramethyl benzidine for horseradish peroxidase neurohistochemistry: A non-carcinogenic blue reaction product with superior sensitivity for visualizing neural afferents and efferents. *J. Histochem. Cytochem.* **26**:106-117.
- Peters, A., S.L. Palay, and H. deF. Webster (1976) *The Fine Structure of the Nervous System*. Philadelphia: W.B. Saunders.
- Ralston, H.J. (1971) Evidence for presynaptic dendrites and a proposal for their mechanism of action. *Nature* **230**:585-587.
- Ralston, H.J., III, and M.M. Herman (1969) The fine structure of neurons and synapses in the ventrobasal thalamus of the cat. *Brain Res.* **14**:77-97.
- Ramón y Cajal, S. (1966) *Studies on the Diencephalon*. E.

- Ramón-Moliner (trans.) Springfield: C. C. Thomas.
- Ramón y Cajal, S. (1911) *Histologie du Système Nerveux de l'homme et des Vertébrés*, Vol. II. Paris: A. Maloine.
- Rustioni, A., and L.C. Ellis (1978) Ultrastructural identification of non-primary afferent terminals in the nucleus gracilis of cats. *Brain Res.* **146**:358-365.
- Saporta, S., and L. Kruger (1977) The organization of thalamocortical relay neurons in the rat ventrobasal complex studied by the retrograde transport of horseradish peroxidase. *J. Comp. Neurol.* **174**:187-208.
- Scalia, F. (1972) The termination of retinal axons in the pretectal region of mammals. *J. Comp. Neurol.* **145**:223-258.
- Scheibel, M.E., T.L. Davies, and A.B. Scheibel (1972a) An unusual axonless cell in the thalamus of the adult cat. *Exp. Neurol.* **36**:512-518.
- Scheibel, M.E., T.L. Davies, and A.B. Scheibel (1972b) On dendro-dendritic relations in the dorsal thalamus of the adult cat. *Exp. Neurol.* **36**:519-529.
- Scheibel, M.E., T.L. Davies, and A.B. Scheibel (1973) On thalamic substrates of cortical synchrony. *Neurology* **23**:300-304.
- Scheibel, M.E., T.L. Davies, and A.B. Scheibel (1976) Ontogenetic development of somatosensory thalamus. I. Morphogenesis. *Exp. Neurol.* **51**:392-406.
- Scheibel, M.E., and A.B. Scheibel (1966a) Patterns of organization in specific and nonspecific thalamic fields. In D.P. Purpura and M.D. Yahr (eds): *The Thalamus*. New York: Columbia University Press, pp. 13-46.
- Scheibel, M.E., and A.B. Scheibel (1966b) The organization of the ventral anterior nucleus of the thalamus: A Golgi study. *Brain Res.* **1**:250-268.
- Scheibel, M.E., A.B. Scheibel, and T.L. Davies (1972c) Some substrates for centrifugal control over thalamic cell ensembles. In T.L. Frigyesi, E. Rinvik, and M.D. Yahr (eds): *Corticothalamic Projections and Sensorimotor Activities*. New York: Raven Press, pp. 131-156.
- Spacek, J., and A.R. Lieberman (1974) Ultrastructure and three-dimensional organization of synaptic glomeruli in rat somatosensory thalamus. *J. Anat.* **117**:487-516.
- Stensaas, L.J. (1967) The development of hippocampal and dorsolateral pallidal regions of the cerebral hemisphere in fetal rabbits. *J. Comp. Neurol.* **129**:59-70.
- Strick, P.L. (1973) Light microscopic analysis of the cortical projection of the thalamic ventrolateral nucleus in the cat. *Brain Res.* **55**:1-24.
- Szentagothai, J. (1963) The structure of the synapse in the lateral geniculate body. *Acta Anat. (Basel)* **55**:166-185.
- Tan, C.K., and A.R. Lieberman (1978) Identification of thalamic projection cells in the rat cuneate nucleus: A light and electron microscopic study using horseradish peroxidase. *Neurosci. Lett.* **10**:19-22.
- Tömböl, T. (1966/1967) Short neurons and their synaptic relations in the specific thalamic nuclei. *Exp. Brain Res.* **3**:307-326.
- Tömböl, T. (1969a) Terminal arborizations in specific afferents in the specific thalamic nuclei. *Acta Morphol. Acad. Sci. Hung.* **17**:273-284.
- Tömböl, T. (1969b) Two types of short axon (Golgi 2nd) interneurons in the specific thalamic nuclei. *Acta Morphol. Acad. Sci. Hung.* **17**:285-297.
- Tripp, L.N., and J. Wells (1978) Formation of new synaptic terminals in the somatosensory thalamus of the rat after lesions of the dorsal column nuclei. *Brain Res.* **155**:362-367.
- Van der Loos, H. (1976) Barreloids in mouse somato-sensory thalamus. *Neurosci. Lett.* **2**:1-6.